

令和 2 年度 博士論文(要約)



**A Method for the Estimation of Muscle
Activation Pattern from sEMG and MRI using
Electrical Network Graph Theory**

(電気回路網のグラフ理論にもとづく表面筋電位と
MRI からの筋活動パターン推定)

指導教員 太田 順 教授

東京大学大学院 工学系研究科 精密工学専攻

学生証番号 37-177238

ピオヴァネッリ エンリコ
Piovanelli, Enrico

**A Method for the Estimation of Muscle
Activation Pattern from sEMG and MRI using
Electrical Network Graph Theory**

by

Enrico Piovanelli

Submitted to Department of Precision Engineering
in partial fulfillment of the requirements for the degree of

Doctor of Philosophy in Engineering

at

THE UNIVERSITY OF TOKYO

September 2020

Certified by

Jun Ota
Professor
Thesis Supervisor

Certified by

Davide Piovesan
Professor
Thesis Supervisor

Accepted by

Jun Ota
Professor
Chairman, Thesis Committee

© Enrico Piovanelli, MMXX. All rights reserved.

The author hereby grants to The University of Tokyo permission to reproduce and to distribute publicly paper and electronic copies of this thesis document in whole or in part in any medium now known or hereafter created.

Except where otherwise indicated, this thesis is my own original work.

Enrico Piovanelli
August 15, 2020

A Method for the Estimation of Muscle Activation Pattern from sEMG and MRI using Electrical Network Graph Theory

by

Enrico Piovaneli

Submitted to Department of Precision Engineering
on August 15, 2020, in partial fulfillment of the
requirements for the degree of
Doctor of Philosophy in Engineering

Abstract

With this thesis I wanted to introduce a novel method for the estimation of muscle pattern activation of forearm muscles using a simple and intuitive modeling based on circuit theory. The model aims to overcome the limitations that were shown by the state of the art methods using electromyography (EMG), magnetic resonance imaging (MRI) and other alternative technique that were proposed during the years. In particular what emerges is the lack of a way for the estimation of deep muscles activation with a time resolution that of the same level of the electromyography. Furthermore, often the morphology of the anatomical sector that is under study is ignored, rather basing the processing on reasonable, yet abstract assumptions.

The method I proposed in this thesis is utilizing a single row of EMG wrapped around the forearm constructing a purely resistive electrical network to describe the volume conductor based on the morphological information that could be directly extracted from the MRI with a set of simple rules. The resulting network could be described with a graph where muscles and electrodes are the nodes and the resistances network is described with a set of weighted edges. The resulting model is linear and describe the relation between the currents on the nodes describing the muscles and the potentials at the electrodes nodes. Because of the way the model is constructed, the description is subject-dependent. The currents on the muscles were then estimated solving an inverse problem exploiting the matricial description of the electrical network that can be obtained with graph theory. The validation of the re-

sulting muscle activation patterns needs to be indirect and is based on criteria on the electrodes space and based on information from anatomical literature. The results shows that the method applied on isometric contractions could provide estimation explaining over 90% of the input information and that have a correspondence with the literature information.

To better understand the relation between the electrodes in specific position and the method's performance for different tasks a study on the influence of the electrodes removal. The issue is approached with the removal of 1 to 3 electrodes and assessing the influence on both the electrode and muscle space. The findings suggests that some of the electrodes could be removed without affecting the results significantly, while parts of the forearm surface are fundamental for the exploitation of the EMG input information. Furthermore the influence on the muscles mainly involved on each task to the electrodes in determined area of the arm was studied, showing that electrodes not directly over the activated muscles are having an influence on the muscle currents estimation

Finally, the method is extended to the dynamic case, with a study on non-isometric movements and introducing the time dimension. The method is applied on windows of the signal and the currents were estimated on simple wrist movements. The results show that the input information could still be mostly explained and the resulting activation are valid solutions, in particular for flex-extension movements of the wrist. Given the simplicity of the proposed model, the calculation time was well under the electro-mechanical delay, proving that its potential application in real time situations.

I believe that this type of new approach, where the morphological information of the anatomy is directly utilized could provide a way to extract additional information from the EMG, with important potential application in the fields of prosthetic and rehabilitation therapy.

List of Publications

Journal Publications by the Candidate Relevant to the Thesis

1. E. Piovanelli, D. Piovesan, S. Shirafuji, B. Su, N. Yoshimura, Y. Ogata, and J. Ota, “Towards a simplified estimation of muscle activation pattern from MRI and EMG using electrical network and graph theory,” *Sensors (Switzerland)*, vol. 20, no. 3, pp. 1–20, 2020, ISSN: 14248220. DOI: 10.3390/s20030724
2. E. Piovanelli, D. Piovesan, S. Shirafuji, B. Su, N. Yoshimura, Y. Ogata, and J. Ota, “Influence of the Number and Position of the Electrodes in the Estimation of Muscle Activation Patterns,” *draft*, 2020

Conference Publications by the Candidate Relevant to the Thesis

1. E. Piovanelli, D. Piovesan, S. Shirafuji, N. Yoshimura, Y. Ogata, and J. Ota, “Muscle Activation Patterns Estimation during Repeated Wrist Movements from MRI and sEMG,” in *The 8th IEEE RAS/EMBS International Conference on Biomedical Robotics and Biomechatronics (BioRob)*, 2020
2. E. Piovanelli, D. Piovesan, S. Shirafuji, and J. Ota, “A Simple Method to Estimate Muscle Currents from HD-sEMG and MRI using Electrical Network and Graph Theory,” in *2019 41st Annual International Conference of the IEEE Engineering in Medicine and Biology Society (EMBC)*, IEEE, 2019, pp. 2657–2662, ISBN: 9781538613115. DOI: 10.1109/embc.2019.8856616
3. E. Piovanelli, D. Piovesan, S. Shirafuji, and J. Ota, “Estimating Deep Muscles Activation from High Density Surface EMG using Graph Theory,” in *2019 IEEE 16th International Conference on Rehabilitation Robotics (ICORR)*, IEEE, 2019, pp. 3–8, ISBN: 9781728127552
4. E. Piovanelli, S. Shirafuji, Y. Ogata, N. Yoshimura, and J. Ota, “sEMG source localization on a three-dimensional model using a Bayesian method: a simulation study,” in *2018 Proceedings of the 2nd International Symposium on Embodied-Brain Systems Science (EmboSS). Osaka, Japan, December 5-6, 2018.*, 2018, p. 36

5. E. Piovaneli, S. Shirafuji, Y. Ogata, Y. Yoshimura, and J. Ota, “A simulation study for visualizing sEMG sources using a Bayesian framework,” in *Proceedings of 40th Annual International Conference of the IEEE Engineering in Medicine and Biology Society (EMBC), July 17-21, 2018, Hawaii, U.S.A.*, 2018

Conference Publications where the Candidate is not first author Related to the Thesis

1. K. Fujikawa, S. Shirafuji, B. Su, E. Piovaneli, and J. Ota, “Estimation of fingertip forces using high-density surface electromyography,” in *2017 International Symposium on Micro-NanoMechatronics and Human Science (MHS)*, 2017, pp. 1–5

Contents

Abstract	ix
List of Publications	xi
Contents	xiii
1 Introduction and Motivations	1
1.1 The problem of muscles' activity estimation	1
1.1.1 Estimation using EMG	3
1.1.2 Estimation using MRI	5
1.1.3 Other approaches	6
1.2 Research Problem	7
1.3 Proposed Approach	9
1.4 Contributions	11
1.5 Thesis Organization	11
2 Neuromuscular System and Control	15
2.1 Introduction	15
2.2 Neuromuscular Control	16
2.3 Methodologies	25
2.3.1 Electromyography	26
2.3.1.1 High Density EMG	31
2.3.2 MRI	34
2.3.2.1 Functional muscle MRI	36
2.4 Other techniques for the estimation of muscle activities	39
2.5 Neuromuscular electrical stimulation	41
2.6 Electrical Network Analysis with Graph Theory	43
2.7 Conclusions of this chapter	49

3	A method for the estimation of muscles activation	51
3.1	Experimental Procedure	52
3.1.1	MRI acquisition	52
3.1.2	HD-sEMG acquisition	53
3.2	Methodology	56
3.2.1	Morphological information segmentation and registration . . .	57
3.2.2	Electric Network Construction	61
3.2.3	Muscles Current Pattern Estimation	66
3.2.4	Validation Criteria	67
3.3	Results	68
3.4	Discussion	74
3.5	Proposed additional validation of the Resistance matrix	80
3.5.1	Methodology	82
3.5.2	Experimental Setup	82
3.5.3	Proposed validation of the system matrix	85
3.5.4	Discussion	87
3.6	Conclusions of this chapter	87
4	Effect of Electrodes Distribution	91
4.1	Introduction	91
5	Dynamic movements case	97
5.1	Introduction	97
5.2	Methodology	98
5.2.1	MRI acquisition	98
5.2.2	Experimental Setup	99
5.2.3	EMG data	100
5.2.4	Segmentation and Registration	101
5.2.5	Electrical Model	103
5.2.6	Muscles' current pattern estimation	104
5.2.7	Validation	105
5.3	Discussion	110
5.4	Conclusions of this chapter	112
6	Conclusions and Future Works	113
6.1	Conclusions	113
6.2	Possible applications and future works	117
	Bibliography	119

Chapter 1

Introduction and Motivations

1.1 The problem of muscles' activity estimation

In the last decades, studies to explore the functioning of motor control gained an important focus for their potential implication not only for medical and diagnostic purposes, but also in the rehabilitation therapy field.

How the central nervous system activates muscles to perform from simple to complex actions is a problem that has not been still completely solved yet, and it still presents unknown components. The mechanism through which the brain is able to control the complexity of the muscle-skeletal system is in fact still topic of plenty of researches. The problem is complicated both from a mechanical and a control point of view due to the inherent redundancy of the muscle-skeletal system. It theoretically allows a broad set of possible solutions making the problem of the estimation of muscle activation and/or forces a challenging and complex topic. The knowledge of the set of muscle activation is therefore an important step to understand the neural strategies used by the central nervous system(CNS) for the planning and

the actuation of the motion.

Different approaches using diverse techniques were proposed for the estimation of muscle activation. Most of the works that can be found in literature exploits a medical diagnostic technique called electromyography (EMG) which is able to record the propagation of the activation potential along the muscles fibers from either the surface of the skin, or from location close to the muscle fibers. It can provide insights on the control information descending from the CNS that is then distributed to the target muscles through specialized structures called motoneurons. Other approaches alternative to the EMG have been presented over the years using different technologies. The introduction of magnetic resonance imaging (MRI), a medical imaging technique thanks to which it is possible to obtain detailed images of inner body structures, allowed the study and the visualization of the metabolic processes that happen during muscle contraction at moderate effort. Other approaches alternative to EMG and MRI were also proposed with the use of other methods that allowed the investigation of the processes happening during muscle contraction, such as ultrasounds and EMG computed tomography. All the described methodologies however, presents some limitations in terms of muscles whose activities are estimated and of recording time resolution, providing incomplete or unsatisfying estimations.

The knowledge of muscle activity is an important information and its estimation is a task worth to be further investigated for multiple reasons. A quantitative measure of the muscle activation is an indispensable knowledge for any study investigating neurological diseases causing muscular malfunctioning. Furthermore, the estimation of muscles activities is a key step in the developing of human-machine interfaces(HMIs) that utilized the muscular intentional information, therefore allowing

a deeper and stronger integration between the human and the machine side. These types of HMI can have an enormous impact in the field of rehabilitation in the form of a stronger mean through which clinicians can get insights and feedback on the muscular process in act. In the field of HMI, improvements of muscle activities estimations could have a particular impact on prosthetic and exoskeletons development, which recently have been gaining a lot of scientific and business interests. A deeper knowledge of muscle activation would allow in fact the development of new control paradigms which better mimic those adopted by the brain.

In the following sections, a summary of the main methods utilized to estimate muscle activities or related measures are shortly described in order to give the reader an initial understanding of the state of the art and of the current challenges. A more detailed description will be later provided in chapter 2.

1.1.1 Estimation using EMG

Electromyography (EMG) is with no doubt the most popular tool for the estimation of muscle activation and muscle forces. EMG can be invasive if it makes use of needles inserted in the target muscle, or non invasive if it uses electrodes attached on the skin above the target muscles. Methods for both types of EMG have been proposed, however the non-invasive use of EMG has particularly drawn focus for its possible application outside the clinical field and for the fact that, unlike for the needle EMG, it does not need any medical staff for its application.

Compared to needle EMG, due to how it is recorded, surface EMG include a higher level of noise. This is due to the fact that for surface EMG there are multiple sources of artifacts, such as power line noise and noise due to muscle crosstalk. This

last type of noise is caused by the fact that the measured information is a noisy mixture of signals coming from multiple sources underneath the electrode position. The influence of noise is particularly evident in recordings using high density EMG (HD-sEMG), a recently introduced evolution of the common surface EMG. High density EMG utilizes dense matrix of electrodes on the skin surface allowing a significant increase in the amount of signal that is recorded but, at the same time, also increasing the amount of noise. This translated into a consequent need of a higher amount of computational power and more advanced analysis protocol.

The growth of HD-sEMG caused a consequent development of an important class of algorithm over the last years for a better and deeper study of undergoing motor control strategies. In particular, the direction of the research using HD-sEMG is toward the development of decomposition algorithms for the extraction of motor unit activity from the mixtures of signals recorded, one example of which are algorithm of blind source separation [9]. The extracted information is specifically the impulse train of the motorneurons that then triggers a sequence of action potentials on the muscle fibers to initiate the contraction. The train of impulses reflects the control signal descending from the CNS through the motorneurons. This information was exploited for practical purposed in subsequent research [10] alongside with the geometric information about the musculo-skeletal system for the reconstruction of movements in impaired people. The impulse train was in fact mapped to an external movements using a simulated musculo-skeletal model properly scale on the anthropometry of the person, for the reconstruction of the intended movements in impaired subjects.

Even though the results obtained are remarkable, these techniques present several

limitations. First of all, they are only able to extract the muscle activity of superficial muscles, therefore ignoring any contribution coming from deep muscles. Even though in the case where only few muscles are present, e.g. biceps and triceps, this could be enough, in the case of other anatomical segments with multiple layer of muscles this actually results in important limitations. It is in fact known that deep muscles have key roles for example in lower back or the forearm. In the forearm in particular, deep muscles form an layer of muscles with important roles for wrist and finger motion. Furthermore, even if most of the methods proposed are based on reasonable assumption on the nature of the signal, they basically ignore the morphology of the anatomical part through which the signal is conducted, rather basing the results of the estimation on the outcome of complex optimization processes.

1.1.2 Estimation using MRI

One alternative method that was proposed for the estimation of muscle activation involved the use of magnetic resonance imaging (MRI). MRI is a diagnostic medical tool for the visualization of anatomical segments and physiological processes happening in the body. It exploits the magnetization properties of hydrogen molecules in the human body to distinguish the different tissues and create a contrast image of the inner structures. It is widely used in medicine for its high resolution properties and the absence of ionizing radiations that instead are present in other imaging techniques (e.g. computer tomography).

The introduction of functional MRI (fMRI) allowed the extension of MRI capabilities for the monitoring of processes happening in the body based on the differences in the blood flow. The fMRI is a well known technique in the field of neuroimaging

for the study of brain activation. However, it has been utilized also for studies involving muscles. The application of fMRI on muscles goes under the name of muscle fMRI(mfMRI) and exploits a difference in the brightness that can be observed in T2-weighted images before and after a sustained effort. It showed important characteristics for the estimation of muscle activation for moderate effort tasks. It overcomes the limitations of EMG for the estimation of deep muscles activation, allowing the estimation of activities of all muscles depicted inside its region of interest. Furthermore, fmMRI results are not influenced by artifacts that are known to corrupt EMG measurements such as crosstalk.

However, mfMRI can only provide information at high spatial resolution, i.e. tenth of millimeters, while the temporal resolution does not allow the quantification of activation dynamics due to the time needed for the task to be executed and the time to obtain the scan as well. Furthermore the need of an MRI makes this method very inefficient from a cost point of view and its cost-effectiveness ratio in fact still remains an unclear point.

1.1.3 Other approaches

Besides works using EMG and MRI, other alternative approaches to the use of sEMG or fmMRI have been presented as well. They exploited other properties of the muscles to assess the activation or the forces that the muscles are applying. These methods span from the use of different well known medical imaging techniques, such as ultrasounds imaging and elastography to the use of other methodologies such as electromuscular stimulation or electrical impedance tomography [11]. Even though some of these methods showed promising results solving some of the problems that

EMG and MRI presented, they have important limitations such as the that given by the size of the instrumentation needed for the data acquisition, as in the case of ultrasonography, or the complexity of the analysis such as in the EMG-CT where a finite element model is needed.

1.2 Research Problem

From the above sections, it clearly emerges that at the state of the art a method that could quantify the activities of all superficial and deep muscles with a temporal resolution comparable with that of EMG (i.e. 1 to 5 kHz) is still missing. The methods using EMG are not able to estimate the activation of deep muscles and the investigation is usually limited to the superficial layer of accessible muscles. The role of deep muscles however, is fundamental, especially in segments where a high density of muscles is observable. One example of such body segment on which I will focus on this thesis is the forearm. The forearm is a very important part of our upper limbs and it includes over 20 muscles that are acting together to allow movements at elbow, wrist and finger joints level. At the state of the art it is not possible to provide information about the activation of the complete set of muscles of the forearm. The use of MRI compensates the limitation in the depth of the investigation, however the intrinsic design of MRI study do not allow to have a time resolution comparable with that of sEMG since the MRI needs to be taken before and after the performing of a motor task which could take several minutes.

One important point that was highlighted in EMG works is the fact that the morphology of the body segments is not considered in the analysis, rather relying on the

outcome of complex signal analysis protocol. In contrast, the anatomical morphology is the key information in MRI studies, which in turn can provide measures only before and after the execution of the motor task (.i.e very low temporal resolution) and are economically burdening due to the cost of MRI acquisition. Therefore a complete study that aims to overcome the limitation of both, would have to successfully be able to merge the electrical activity information with the anatomy description that can be extracted with technique such as the MRI.

Even though several attempts were made, at the state of the art, there are no works that manage to successfully merge the high temporal resolution information that could be obtained from EMG with the anatomical description that could be assessed from an MRI for the estimation of the muscle activation pattern for the whole spectrum of muscles, i.e. both superficial and deep muscles. There is therefore the need of a method that could map the EMG information into a morphology described with the use of imaging technique in order to successfully integrate the two types of information to obtain a complete knowledge about the activation status of muscles. In this thesis I will propose a solution method focusing on the study of the forearm due to its high number of muscles that populates it and to the importance that these muscles have in our everyday life and in the development of human manual skills.

The high muscle density in the forearm requires the use of a higher number of electrode in order to be able to collect all the information needed. However a higher number of electrodes would concurrently increase the processing required for the extraction of the useful information, therefore limiting a potential application for example in the prosthetic field, where a lower number of electrode is preferred.

Therefore it will be important that the proposed solution include a contained number of electrodes, enough to collect the required information from the high number of muscles but not excessive in order to not burden the processing phase. Moreover, considering the high number of electrodes it is important to evaluate the robustness against electrodes shifts or eventual malfunctions. In particular it is important to determine how the methods performance are changing with the number and the positioning of electrodes and how the density of the electrodes is influencing the outcomes. As a consequence, with the perspective of a possible future application, the ease of electrodes application is an important issue and therefore, evaluating the robustness to different configurations and to different type of motor task are hence important criterion for the evaluation of the methods applicability in real contests.

1.3 Proposed Approach

Considering the requirements that emerges from above considerations, in this thesis I propose an approach different from what have been proposed before, aiming to find a better merging between the EMG and the morphological information to investigate the muscle activation pattern on the forearm muscle set. In particular, the proposed approach exploits the circuit theory to provide a simple description of the volume conductor and to define a network able to describe the current path from each muscles to the electrodes on the skin.

Therefore, considering the described motivations, with the work of this thesis I aimed to answer the following questions:

- Is it possible to estimate the muscle activation of an anatomical segment with

a high number of muscles at different depth?

- Is it possible to treat an anatomical section of the forearm analogously to a power grid and see the system as a simple current divider that can be solved using circuit theory?
- Is it possible to exploit the morphological information that can be taken from imaging techniques to improve the estimation?
- How could the method be validated non-invasively?
- How robust is the proposed method to a limited number of missing electrodes and how these are influencing the performance in terms of quality of the estimation and of percentage of information explained?
- What are the location where it is crucial to have electrodes placed and which other could have instead a lower density of electrodes?
- How accurate is a resistive model to describe the signal propagation in the human tissues?
- Is the method extendable to dynamic tasks?
- Is the processing time needed by the method allowing it a real time computation?

1.4 Contributions

With regards to the research queries described, the investigation carried on for this thesis allowed to clarify the following points:

- Developed a method for the estimation of muscle activation pattern exploiting morphological information and EMG information.
- Tested the method for isometric tasks involving the wrist and the fingers joints.
- Assessed the robustness of the method and the influence on the method performance of the electrodes positioning and number.
- Proposed a partial validation of the model using a direct electrostimulation of the muscles.
- Extended and tested the method to dynamic movements.

1.5 Thesis Organization

The thesis will be organized according to the following chapter division

1. **Chapter 2 - *Neuromuscular system and control*** : In this chapter background information about the neuromuscular system are described. In particular the anatomy and the description of the central nervous system is presented and how the theories behind motor control strategies are explained. A description of the methodologies to access the information (electromyography) and the

anatomy (magnetic resonance imaging) of the central neural system is reported afterwards, with a deeper focus on the HD-sEMG and fmMRI. Furthermore a brief description of the state of the art in the algorithms for the estimation of muscle activities using EMG, MRI and other alternative methods are thoroughly described. A short introduction into the techniques of electromusculo stimulation is provided as well, as long as the different types and applications in which it has been utilized. Finally a short introduction into the circuit theory to solve linear resistive circuit, as long as the graph description of the tools for the circuit analysis is provided.

2. **Chapter 3 - *A method for the estimation of muscles activation*** : In this chapter the method is presented with an explanation on how the model describing the relation between the muscle activation and the measured EMG is constructed along with the method for the estimation of the muscles activation pattern. The method is tested on 4 healthy participants repeating 4 type of different isometric tasks on the wrist and on the metacarpophalangeal joint of the middle finger at different force levels. The validation is done on the electrodes space and on the muscles space, comparing the reconstruction of the voltage on the electrodes with the measured sEMG and comparing the obtained muscles' current pattern with specialized medical literature on the muscle involved. Additionally, an supplementary method for partial model validation is proposed using electric muscle stimulation to validate the resistive network composing the model.
3. **Chapter 4 - *Effect of Electrodes Distribution*** : In this chapter the effect

of the electrodes distribution are presented. The robustness of the method to different configuration is assessed evaluating the effects on the method's performance of the removal of variable numbers and configurations of electrodes. The effects are evaluated both on the electrodes and on the muscles' current space to have a complete understanding.

4. **Chapter 5 - *Dynamic movements case*** : In this chapter the study is extended to the application of the method to dynamic movement, in order to discuss results with a higher application relevance. The method is applied using a windowing to observe its behavior on time. A further refinement with the application of Bayesian inference for the estimation of the currents will be done in the future.
5. **Chapter 6 - *Conclusions and future works*** : In this chapter a general discussion of the topics covered in the thesis, the limitation of the methods as well as the future possible development and application in the field of medical therapy and rehabilitation engineering are described.

THIS PAGE INTENTIONALLY LEFT BLANK

Chapter 2

Neuromuscular System and Control

2.1 Introduction

A wrist flexion might seem like a trivial task, something easily performed every day. However, that simple task is the results of a very complex sequence of planning events that starts from the brain and end with the controlled contraction of a set of muscles that has a torque on the wrist joint as result. The control of the human movement is a complex task that involves multiple structures. The command originates in the central nervous system (CNS) and propagates to the target muscles to initiate their movements. The redundancy of the musculoskeletal system makes the planning of the movements a challenging task, and still an exact explanation on how the CNS overcome this inherent redundancy was not found. Studies on the neuromuscular system are an important branch of the modern biomedical engineering research. In

particular research investigating the muscular system and control gained considerable attention for the potential effect that their finding might have in the medical and rehabilitation fields. A common way of intercepting the motor command to access the neural information is the use of the electromyography (EMG). Plenty of studies were conducted with the use of EMG for the extraction of relevant information of different nature. The recent introduction of high density EMG further broaden the field of investigation of the EMG studies. While EMG is an important method to access the neural descending information, the morphological information also has an important meaning in the studies of the motor control. The most efficient method to depict the internal structure of body parts is the Magnetic Resonance Imaging (MRI). A particular type of MRI called muscle functional MRI was proposed to estimate the activation of muscles during sustained motor activities. This chapter contains the description of the neuromuscular system and how it controls the contractions of the muscles to perform a desired task. A detailed description of how the EMG and the MRI techniques work follows, with a description of the most recent techniques for muscle activation estimation, with a particular focus on separation methods on HD-sEMG data and fmMRI. Finally a description of the electromuscle stimulation methods and application and a short explanation of circuit theory and circuit analysis for resistive networks are provided.

2.2 Neuromuscular Control

The system and the neural strategies that regulates voluntary movements are usually referred as neuromuscular control. The neuromuscular control originates from the

brain and involves all the structures that bring its signal to the target muscles. In particular the brain, the brainstem and the spinal cord compose what is usually referred as the central nervous system (CNS). The CNS is responsible to process and integrate proprioceptive and sensory information to control and plan the desired motor tasks. The signal transmitted to the muscles is the results of a complex integration process where excitatory and inhibitory inputs are summed at different points along the path from the brain to the muscles. The motion command is first generated on the brain, in particular in the primary motor cortex, which is the main responsible region for motion control. Different areas of the primary motor cortex are activated concomitantly to specific limb movements. Information from other regions of the brain, functionally connected to the primary motor cortex, is also integrated for the generation of the motor command. The resulting signal is in turn transmitted through specialized neurons in the spinal cord, called upper motor-neurons. Upper motor neurons are then forming synapses with lower motor-neurons in the spinal cord. Lower motor-neurons integrate information descending from upper motor-neurons and from sensory receptors to then generate a signal transmitted directly to the target muscles to initiate the contraction (Figure 2-1).

The axons of multiple motor-neurons leave the spinal cord and group in structure called nerves. Each of the axons of the motor-neurons in the nerve is also referred as nerve fiber. From the nerve bundle, the nerve fibers spread to different location in the body. When reaching the target muscle, each nerve fibers then branches to innervate multiple muscle fibers, one per branch. The muscle fibers innervation points are usually concentrated in a limited volume portion of the muscle called innervation zone. The set of a motor-neuron and the muscle fibers that it innervates,

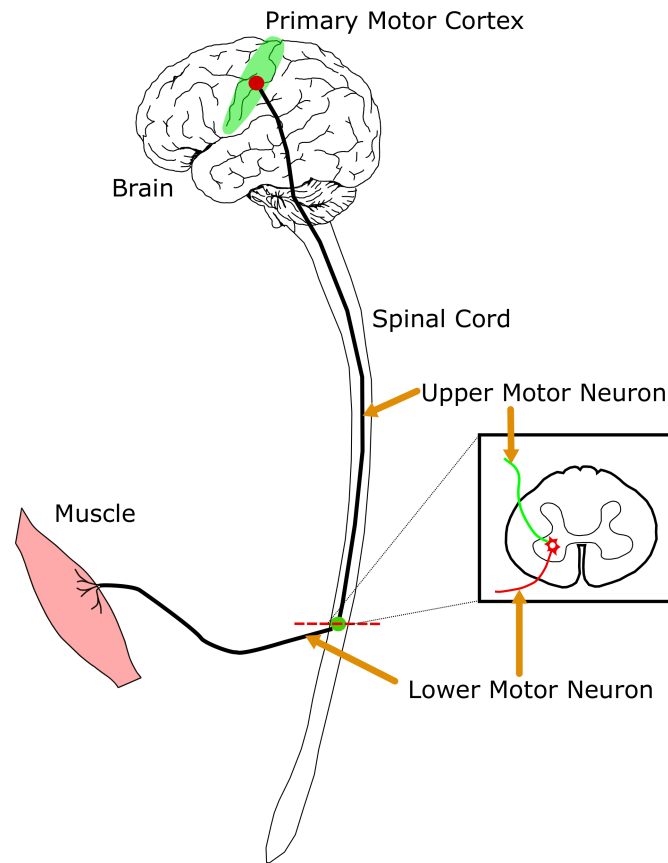


Figure 2-1: Path of the motor signals from the primary motor cortex region in the brain to the target muscles.

are defined as motor unit. Motor units are considered the fundamental functional units in the human motion control. The muscle fibers of a motor unit are distributed in a subvolume inside the muscle volume which, depending on the type of muscle, can occupy from 10% to 70% of the cross sectional area of the muscle[12].

The signal that is transmitted from the brain to the muscles is called action potential and has a characteristic shape (Figure 2-2a). An action potential is a rapid fluctuation in the polarization between the intracellular and the extracellular fluid of a neuron. It is characteristic of electrically active cells, such as neurons and muscle cells. The potential difference at rest across the membrane of a neuron is maintained constant at a value of -70mV to -80 mV, usually referred as resting state potential. In this state the ionic channels in the membrane are closed and allow to maintain the resting state potential. An action potential is triggered only if a depolarization reach a defined threshold value. If that voltage value is reached, voltage-dependant ionic channels open causing the migration of sodium ions (Na^+) in the intracellular fluid through the membrane with a consequent depolarization of the trans-membrane potential. When the peak depolarization is reached, the re-polarization starts with the closing of sodium channels and the opening of potassium gates that cause the flow of potassium ions (K^+)ions to the extracellular fluid. Re-polarization is followed by a refractory period where the sodium and potassium channels are closed and the membrane return to the resting state. During the refractory period it is impossible for incoming action potential to trigger a new action potential, hence the definition of refractory period. The length of the refractory period set a limit to the frequency of action potential firing. The duration of an action potential differs with the type of cell that is firing it. Action potentials on neural cells are faster than those happening

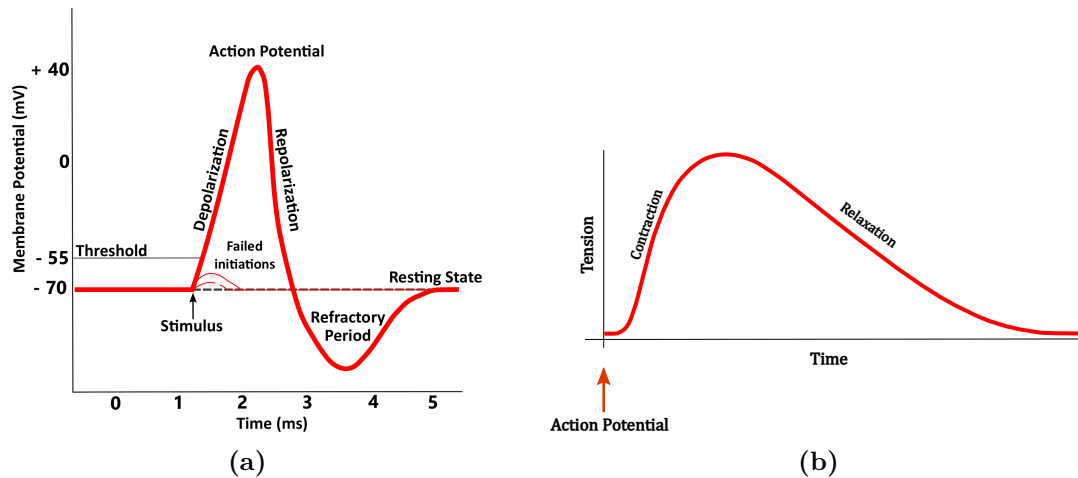


Figure 2-2: (a) Action potentials of a neuron. It is possible to observe the 3 different phases that characterize the voltage fluctuation. (b) Muscle twitch obtained with a single action potential.

on muscle cells.

A single action potential on a motorneuron elicit a force generation called twitch (Figure 2-2b). While an action potential has a positive and a negative phase, a twitch only has a positive phase. Different type of fibers presents different types of twitches.

The point where the axon of the motorneuron create synapses with the muscle fiber is called neuromuscular junction. When the action potential reaches the neuromuscular junction, a neurotransmitter is released in the synaptic junction causing the onset of action potentials in the muscle fiber that propagates away from the neuromuscular junction in both directions along the muscle fiber. When the action potential flow through the muscle fiber it causes the release of calcium ions in the muscle cells inducing the initiation of the contraction. The contraction of a muscle

fiber is possible thanks to the interaction of two contractile proteins that constitute all muscle fibers: actin and myosin. The interaction between these two proteins and adenosine triphosphate(ATP) allow to convert chemical energy into mechanical energy. Muscle fibers are built as a sequence of repeating elements called sarcomere. A sarcomere is the fundamental force generating unit of muscles. It is bounded by 2 Z-disc defining a volume where actin and myosin are properly arranged(Figure 2-3). Actin and myosin can form bonds called cross-bridges and the process of creation of a actin-myosin link is called cross-bridge attachment while the revers process is called cross-bridge-detachment [12]. When myosin molecules bind ATP molecules they undergo a transformation process that cause a sequence of cross-bridge attachment, pulling action and cross-bridge detachment. The pulling action brings the z-discs closer to each other resulting in an overall shortening of the sarcomere. The cycling of this attachment-pulling-detachment process is the responsible for the fiber's production of force.

The number of action potentials measured on a muscle fibers is correlated to the muscle activation. However the linearity is only guaranteed under specific conditions and is disrupted in presence of circumstances such as muscle fatigue [14]. In fact when the muscle is under fatigue conditions, its force generation capacity decreases and the association between the number of action potentials and muscle force is not valid anymore. During fatigue the peak twitch shape change with a decrease in the force peak and an increase in the duration having as a consequence the exertion of a lower force and with a slower response. Another factor influencing the linearity of the action potential-force relationship is the dependence of the exerted force on the activation history of the muscle. In fact it was observed that a muscle twitch

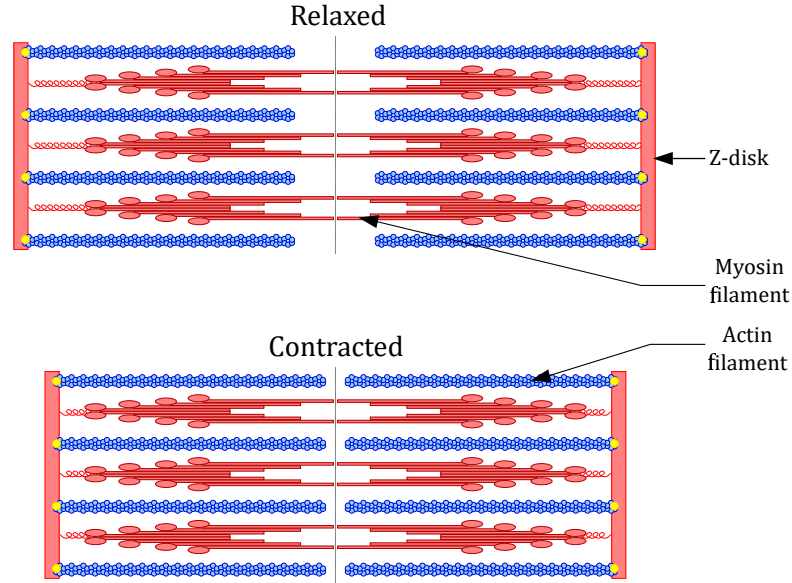


Figure 2-3: Sarcomere as fundamental force generating unit. Modified from [13]

generated from a single electrical stimulus has a higher peak immediately after a maximum voluntary contraction. This phenomena is called post-activation potentiation [15]. Furthermore, the maximal muscle force depends also on the rate of change of muscle length. It decreases as shortening speed increase and conversely increases as the muscle is lengthened. The reduction of the muscle force with an increase in the shortening velocity is caused by an increasing number of missed cross-bridges as the filaments slide in the sarcomeres, causing a reduction of the average work performed. Conversely, the increase of the maximal force when the muscle is lengthening is due to an increase in the amount of calcium ions released in the muscle cells that causes a higher work performed by each of the cross-bridges.

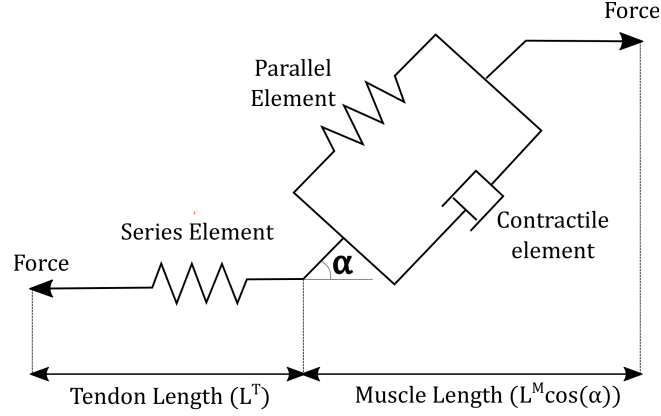
The CNS can modulate the output muscle force through two possible strategies:

- changing number of motor units recruited (recruitment)

- changing the firing rates at which the action potentials are discharged (rate coding)

Force modulation through motor units recruitment is a modulation strategy that mainly acts at low level force while rate coding occurs at higher force or during fast contractions. The two strategies however, happen and work together. Motor units tend to be recruited in the same order during voluntary contraction [16–18] according to a size principle. That means that motor units innervating smaller and weaker portions of fiber tend to be recruited first and vice versa, motor units innervating bigger and stronger set of muscle fibers are progressively recruited as the effort continue or increase. The threshold for the recruitment of motor units has an exponential shape with respect to an increase in the needed force. Therefore most of the motor units are recruited at low force level, and as the force level increase few motor units can be recruited. For this reason the modulation of force of high rate is mostly related to a change in the discharge rate.

When the contraction starts, the force exerted from the muscles is not directly applied to the skeletal system, but it is transmitted to the bones through connective tissue segments. These connective tissue parts comes in the form of either bundles of connective tissues called tendons or connective tissue sheets called aponeurosis which are in turn attached to the bones. The proximal site of attachment of the tendon is called origin while the distal point of attachment is called insertion. Origin and insertion of a muscle are located at the opposite sides of a joint and when force is applied during muscle contraction it can cause a rotation or a sliding at joint level[12]. Muscles and tendons together define a muscle-tendon unit (MTU). Properties of MTUs can be modeled with a mechanical system, the most famous of

**Figure 2-4:** Hill's model

which was developed by Hill [19] and is often referred as Hill's model. Based on his model, a lot of other models were subsequently developed and they go under the name of Hill type models [20, 21]. The Hill's model is represented in Figure 2-4

MTU models are fundamental elements in models of the musculoskeletal systems. These models, called musculoskeletal models, are used in simulated environment for the estimation of muscle forces and joint torque for the study of the behaviour of the musculoskeletal system[22].

Musculoskeletal models are simulated models that represents the human musculoskeletal apparatus, where muscles are modeled as MTU and can be considered the actuators applying for once the skeleton, the system frame. They are used to solve kinematic and dynamic problems happening in the human body since they can model the high number of degrees of freedom (DOFs) of the musculoskeletal system to describe the complexity of movements that a human can perform. The number of muscles is usually in a higher number compared to the DOFs controlled, making the human musculo-skeletal system a mechanically redundant system[23]. This means

that the solution space of the control problem that the CNS has to solve to plan a motion is theoretically infinite. The understanding of how the CNS can generate a pattern of muscle activation to achieve a particular task has been the topic of important research in the field of neurology.

The most prevalent solution is the muscle synergy theory[24]. It states that the CNS reduces the space of control signal using a combination of a smaller set of fundamental invariant blocks called synergies. Muscle synergies represents a fixed pattern of activation of muscles that are scaled, delayed and combined to create the muscle pattern that allow the target movement to happen as planned.

The origin of muscle synergies is still a debated topic. Even though most of the works support a neural origin of muscle synergies [25, 26], other works suggested that other components might have an influence in the definition of muscle synergies [27], stating that the synergies might have also a component due to the mechanical constraint of the system. This de facto suggest that, all the muscles involved are necessary for the movement, even if their involvement is apparently not significant. Given these evidences, current theories move toward a hybrid explanation for muscle synergies.

2.3 Methodologies

In this section the most common techniques utilized for the study of the neuromotor system are described in detail. A particular attention is payed to electromyography and magnetic resonance imaging, two of the main tool adopted for the investigation of the mechanism by which the CNS plan human motion and for the exploration

of the phenomena occurring at muscular level during contraction, and the two tools that I will be using for this thesis. In particular, the application of EMG and MRI specific for the study of muscles i.e. high density electromyography (HD-sEMG) and muscle functional MRI(mfMRI) are described. A summary of the most critical features of the main described techniques is schematically reported in Table 2.1.

Table 2.1: Table with some of the most important features characterizing surface EMG, intramuscular EMG and mfMRI.

	surface EMG	intramuscular EMG	mfMRI
Deep muscles estimation	NO	YES	YES
Noise & artifacts influence	YES	NO	NO
Time resolution	HIGH	HIGH	LOW
Space resolution	HIGH	LOW	VERY HIGH
Setup cost	LOW	LOW	HIGH
Need of medical personnel	NO	YES	YES

2.3.1 Electromyography

Electromyography(EMG) is an diagnostic technique that record the electrical activity produced by muscle fibers as a consequence of the depolarization occurring on their membrane. EMG is used in the medical field to identify diseases or abnormalities affecting the neuromuscular system. It is also applied to record the signal used to control external devices such as prosthetic limbs.

EMG can be recorded invasively and non invasively. Non invasive EMG, usually referred as surface EMG (sEMG), uses electrodes placed on the surface of the skin to collect the potential signal generated by muscles. Invasive EMG collects the muscle signal from location in proximity of the target muscle through the use of needles.

EMG signal is generated by the electrical activity of the muscle fibers active during a contraction. The depolarizing and re-polarizing zones of the muscle fibers are acting as sources moving along the fiber. The tissue separating the source and the recording site is called volume conductor. Its properties largely determine the features of the detected signal (e.g. frequency content). The volume conductor act as a spatial and temporal low-pass filter on the potential distribution. For intramuscular reading the effect of tissue is lower since the reading point is very close to the source [28, 29]. The volume conductor effect is therefore mainly observable in surface electromyography and is mainly spatial, causing a distortion of the motor units' potential waveform. The EMG readings can be then considered a mixture of a higher number of sources compared to the intramuscular EMG.

During a surface EMG recording, the signal produced in the source propagates through the volume conductor and arrives to the electrodes. Since the potential of a MU is propagating through the volume conductor, the characteristics of the volume conductor can strongly influence the quality of the detected signals. In fact, the surface EMG recordings depends on different parameters not only of the anatomical physical component (i.g.volume conductor), but also on parameters of the detection system. The factors that can influence the EMG signal are multiple:

- the thickness of the subcutaneous tissue layer
- the depth of the source within the muscle
- the distance of the source from the electrodes
- the inclination of the detection system with respect to the muscle fiber orien-

tation

- the length of the fibers
- the location of the electrodes over the muscle
- the spatial filter used for signal detection
- the inter-electrode distance
- the electrode size and shape
- crosstalk among nearby muscles

Out of these many parameters, crosstalk is particularly important because it is a significant source of noise for surface EMG. Crosstalk is a type of artifact that leads to a corruption on the signal that is detected over a certain muscle caused by other nearby muscles. It usually happens when the distance of the detection points from the sources is of the same order of magnitude for the sources in different muscles, causing multiple signals to overlap with similar amplitudes. It is one of the most important source of error that lead to the misinterpretation of the surface EMG.

The use of surface EMG gained a lot of attention for being completely non invasive and easy to use. Manifold studies were conducted using surface EMG, with different purposes such as application in rehabilitation [30] or for the assessment of conduction velocity[31]. However, even though normal surface EMG demonstrated to be useful in many field and for many studies, it presents important limitation, particularly for investigations targeting the behavior of single motor units. Additionally, surface EMG requires a careful placements of the electrodes on the target muscles in order

to reduce the crosstalk, and misplacement can introduce important fluctuations in the variables estimated with the EMG [32].

EMG information is mainly used to estimate the activation level of muscles. The choice of surface or intramuscular EMG mainly depends on the anatomical section that is being target by the study. However the use of surface EMG is more common since it can be done in a research laboratory without the need of trained personnel and a sterile environment.

Most of sEMG studies require a quantification of the muscle activity. For this purpose different approaches were proposed over the year. When surface EMG is collected with a single channel i.e. using monopolar or bipolar electrodes, these are attached on the skin over the target muscles according to specific standard and indications that allow the minimization of cross-talk effects. In this way it is assumed that all the signal recorded on that electrode is coming mostly from the muscle underneath. However the EMG often need a denoising step before undergoing further processing in order to clean it up from any possible artifact that might corrupt it. Multiple technique exists to denoise the signal, such as Wavelet decomposition, independent component analysis and higher order statistics. The proper use of these techniques can significantly reduce the amount of noise affecting the measurements[33]. Once cleaned, muscle activation can be estimated with several methods. The main ones are those from the EMG amplitude and those from the analysis of the frequency domain of the EMG signal.

After the signal is cleaned from unwanted components, for the estimation of muscle activation from surface EMG amplitude, the signal is usually processed according to a series of stages : whitening, demodulation, smoothing and relinearization

[28]. The whitening process, temporally uncorrelates the EMG samples. In fact successive EMG samples are normally correlated and the this temporal correlation create an uneven temporal "weighting" on the information, that after the whitening is flattened[28]. Demodulation and relinearization are stages that are connected. Demodulation aims to estimate the signal standard deviation from the EMG samples. In order to do so, at this stage either the absolute value or the square of each of the sample is calculated. Relinearization changes based on the type of demodulation applied : if the absolute value was used, the relinearization is not necessary, if the samples were squared during the demodulation, the relinearization consists in the application of a square root to all samples. The mean of the resulting signal is equal to a scaled version of the original signal's standard deviation. The smoothing stage apply a low filter on the demodulated signal to remove the inherent fluctuation inside the EMG signal. It can use an averaging window of a properly calibrated lenght or other linear low-pass filters. The signal resulting from this processing is an estimation of the standard deviation of the EMG signal contained in the recorded data. This type of signal has been used for many years as control primitive for myoelectric prosthetics

An alternative way to assess muscle activity using EMG is the use of properties of the frequency domain. In particular they are based on the observation that the frequency spectre of the EMG changes with the contractions. A large number of studies were done on the frequency domain of the EMG. Important studies showed the correlation between the manifestation of muscle fatigue and the shift of the EMG spectre [34]. Additionally other studies utilized spectral analysis with techniques such as STFT during voluntary isometric contractions or during electrically elicited

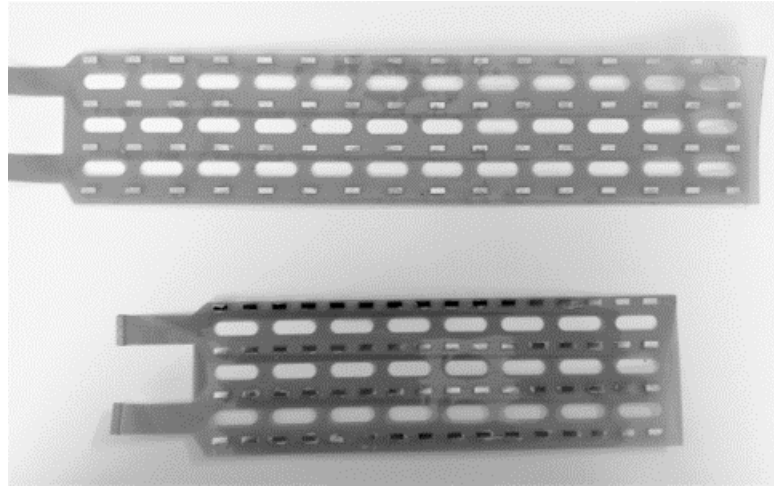


Figure 2-5: Example of high-density EMG electrodes sheets

contractions to detected changes in the muscle responses. The study of the sEMG signal on the frequency domain is however out of the scope of this thesis.

2.3.1.1 High Density EMG

In order to overcome some the limitations of the normal surface EMG a new type of EMG was recently introduced. It is called high-density sEMG(HD-sEMG) and it records the muscle potentials with matrices of densely placed electrodes covering a surface over the target muscles (Figure 2-5).

The use of HD-sEMG provides a set of data with a higher spatial sampling and a higher spatial filtering, allowing a better discrimination power to distinguish action potentials coming from different motor units[29]. In fact HD-sEMG record the signal no more from a single position, but from a surface, therefore adding one spatial dimension to the data, i.e. the signal recorded has 2 spatial dimension and

one time dimension. This significantly increase the amount of information collected but it concurrently burden the time needed for processing.

The additional dimension in the data allow to perform analysis of EMG that creates maps that give indirect information about the spatial recruitment of motor units within a muscle [35]. These maps allow the monitor the localization of the active areas of the muscles underneath the electrodes, and, thanks to the high time resolution of EMG, it is possible to observe the different activation timing of muscles.

One important task that HD-sEMG allowed to explore is the activation pattern of single motor units. The problem of extracting information about the motor units activation from common surface EMG is a difficult task that often brings to erroneous conclusions [29, 36]. The low selectivity of the system in fact make it difficult to clearly distinguish the action potentials from different sources. Therefore the need of higher spatial resolution in the recordings in order to discriminate different action potentials shapes. A higher spatial resolution, i.e. a higher number of electrodes, comes however to the cost of a considerably higher amount of information collected with a consequent need of advanced signal processing technique that could exploit the characteristics of the multi-channel recordings(e.g.time structure, mutual information, statistical properties).

One way to improve the extraction of motor units activation from the HD-sEMG is to exploit the additional dimension of the recorded information applying a spatial filter. Spatial filters are linear combination of neighbor signal values that improve the selectivity of the recordings [29]. They allow to reduce the number of motor units influencing the recordings and to discriminate the different action potentials. The shape of spatial filters define the selectivity of the filtering process and it de-

depends on the application and the processing technique[37]. Highly selective spatial filtering can significantly help discrimination algorithm based on the shapes of the action potentials, while blind source separation algorithms are not influenced by such processing.

This last category of separation algorithm are actually the most algorithm utilized in the state of the art works. The interference signal nature of the information collected with HD-sEMG make the application of blind source separation (BSS) algorithm an intuitive choice for the extraction of the underlying motor unit activation.

Holobar et al [38, 39] proposed a blind source separation method called convolution kernel compensation (CKC) for the extraction of the input impulse train of a multiple input-multiple output (MIMO) system. The method assumes a low probability of overlapping pulses, therefore searching for weakly correlated and highly sparse solutions. No prior probability density function is assumed on the impulse trains. CKC showed to have performance comparable with the linear minimum mean squared error (LMMSE) estimator, which is the optimal Bayesian estimator for linear mixing systems.

Improvements and modification of the CKC were proposed afterwards, such as the Gradient CKC [40] where the unknown mixing matrix of the linear system modeling the mixture is compensated in order to be more efficient in realistic cases where recordings are low-quality noisy signals.

Recently Negro et al[9] combined different blind source separation approaches already presented [38, 41] into one general framework, proposing a robust validation with comparison with the gold standard of experts from invasive recordings and a validation using the two sources approach [42]. The resulting convolutive blind source

separation algorithm proved to have high performances in a variety of conditions.

The convolutive blind source separation algorithm proposed by De Luca et al. is the state of the art for the extraction of motor units from the interference signal recorded with HD-sEMG and was recently applied into the protocol for recent work with different purposes [43–45].

Even though the capabilities of the presented algorithms are remarkable, they present important underlying limitations. The most important one is the inability to assess the activities of the deep muscles. In fact the motor unit train pulses are only assumed to come from the superficial muscles and the effect of the deep muscles is ignored in the analysis. Furthermore it is not clear whether it is possible to assign the estimated motor units to the different muscles if there is a high number of muscles under the electrodes sheet, therefore it is not possible to discriminate the position of the sources estimated with the separation algorithm. Finally, all the decomposition algorithm rely their processing exclusively on mathematical assumption, ignoring however information about the underlying morphology and the anatomy of the volume conductor, i.e. the arrangement of the muscles, their size and shape.

2.3.2 MRI

Magnetic Resonance Imaging (MRI) is a non invasive medical imaging and diagnostic technique that allows the visualization of inner morphological structures. It utilizes a strong magnetic field, a magnetic field gradient and radio frequency (RF) waves for the generation of images of anatomical structures.

MRI is possible because of the magnetic properties of hydrogen nuclei which give them a non-zero magnetic moment. When hydrogen nuclei are placed in a strong

constant magnetic field (B_0), they align to the magnetic field direction z and they start precessing at its frequency to minimize their energy. The application of an RF pulse (B_1) of a set amplitude and time can change the net polarization of the molecules so that it flips to the transverse plane xy and to come into phase with the RF pulse. The transverse component of the nuclei induces a detectable magnetic signal that is generated and recorded on a receiver coil.

After the RF pulse cease, the nuclei will start realigning with B_0 i.e. move to a lower energy state, losing phase coherence on the transverse plan and emitting the energy absorbed in a process referred as relaxation [46]. During relaxation 2 parameters can be calculated :

- **T1 or longitudinal relaxation time:** time necessary for the longitudinal component of the magnetization along B_0 to recover. T1 is a constants of time defined as the time in ms necessary for the magnetization to recover 63% of the final value.
- **T2 or transverse relaxation time:** time necessary for the transverse component of the magnetization along B_1 to decay. T2 is a constants of time defined as the time in ms necessary for the magnetization to reach 37% of the initial value.

The human body contains a significant amount of water, and therefore hydrogen nuclei, and is particularly concentrated in tissues and in fat. Each different type of tissue recover the equilibrium state after the RF perturbation with a different relaxation process of T1 and T2[47]. The use of T1 or T2 time and the use of one or the other time for imaging allow to highlight different structure. In particular

T1-weighted images are used for visualizing cerebral cortex, fat tissue and in general to obtain morphological information, while T2-weighted images are used to detecting edema and inflammation and for white matter lesions [47].

In commercialized MRI scanners the main body of the scanner contains the coils for the generation of the B_0 uniform field, the gradient system for the localization of the scanning regions and the system for the generation of the RF pulse. The subject is laying down on a sliding table that is then moved into the scanner bore during the scan. Depending on the body part that need to be analyzed a receiving coil is utilized to read the magnetic signals.

MRI can be used to also visualize processes that are happening in the tissues when performing some tasks. This use of MRI is usually referred as functional MRI (fMRI) and it is widely used in the field of brain science to visualize the areas of the brain involved in specific tasks.

2.3.2.1 Functional muscle MRI

In the studies of muscles there is a less known type of fMRI, namely muscle fMRI (mfMRI) which exploits the difference in T2 relaxation time between rest and after exercise. It has been in fact shown that the after exercise the T2 relaxation time of muscle water increase, causing an increase of the signal in T2-weighted images[46, 48]. Therefore muscles that are activated during specific exercise will be visualized with a brighter color with respect to a scan taken while resting. mfMRI studies were proposed to investigate different part of the bodies (lumbar muscles[49, 50], triceps surae [51], hip abductors [52], upper arm [53]) and exercises (plantar flexion [54]).

It has been demonstrated that there exist a linear relationship between the forces

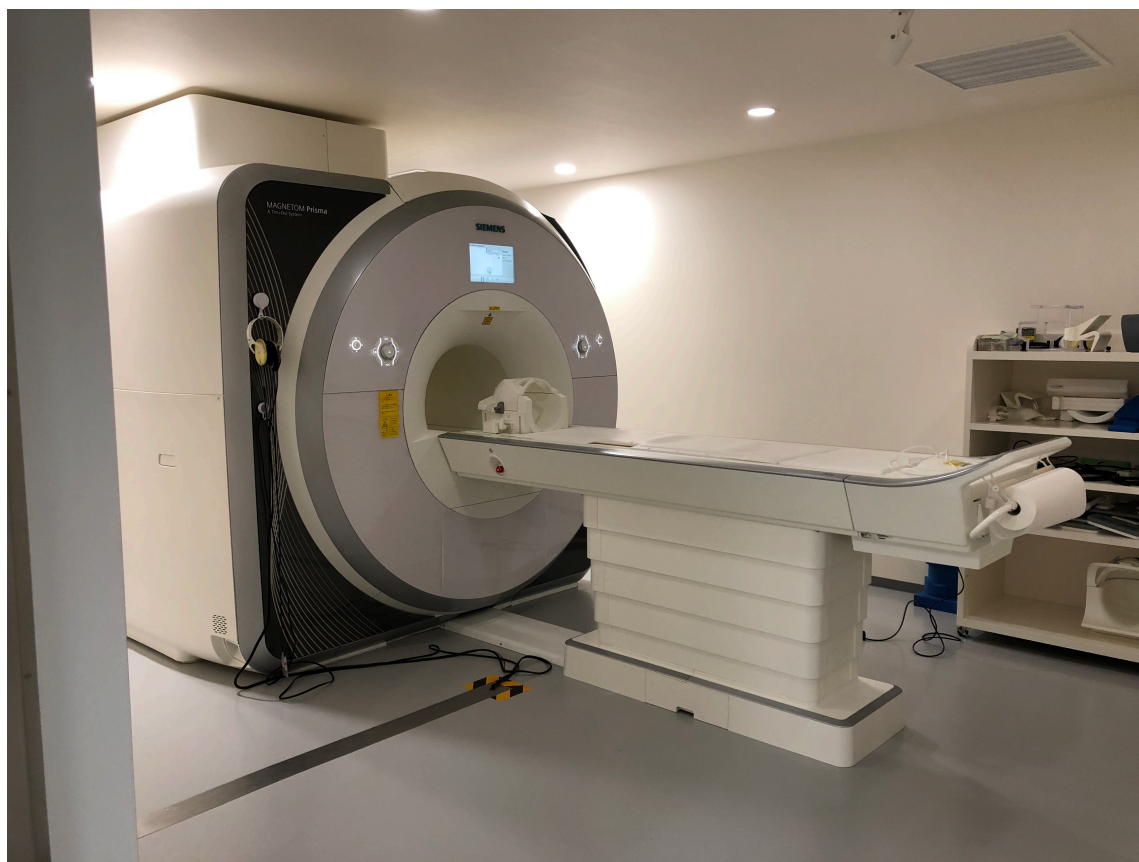


Figure 2-6: Example of MRI scanner (Siemens, Germany)

exerted during exercise and the increase in signal observed in T2-weighted images for moderate levels of muscle activation [50, 55], while lower and high intensity activities disrupted the linearity [49] supporting more a sigmoid shaped relationship between force and activation. Experiments comparing EMG and mfMRI showed the presence of a consistent relationship, even if not always between the two methods provides different outcomes. The reason for this discrepancy is allegedly reflecting the different physiological origin of the information that EMG and mfMRI capture[46]. In particular EMG provides information about the electrical activity of muscles, while mfMRI reflects the metabolic activity of muscle tissues.

Even though mfMRI and EMG provides comparable information, mfMRI presents some important advantages. It is a non-invasive technique that can record information of multiple information with a single scan. In particular, differently from EMG, it can record activities of deep muscles non-invasively and without artifacts that are usually corrupt EMG recordings such as crosstalk.

However, due to their intrinsic experimental design mfMRI studies are limited to study spatial information and not the temporal information. In fact mfMRI scans need to be taken before and after specific exercise and therefore the time resolution is very low and delays needs to be considered for the fact that mfMRI is a post-exercise technique. Additionally, as stated before, mfMRI provides most of the meaningful results at moderate force effort, while low and high force exercises actually provides less solid conclusions. Finally mfMRI requires the use of an MRI scan with consequent higher costs and times, therefore limiting its practice only to research laboratories. The mfMRI showed important characteristics, first of all its capacity to access information of deep muscles non-invasively and without the use of

any further data processing. However, even it is a promising technique, its feasibility in terms of cost is still not clear.

2.4 Other techniques for the estimation of muscle activities

A summary of the major researches for the estimation of muscle activation or other information related to muscle activity, such as the MTU impulse train, was presented along with the description of the techniques that mainly contributed to progress in the study of muscle behavior and motor control.

Even if less known, alternative techniques were tried for the quantification of the muscle activation or of other quantities related to them. In this short paragraph I will list up the main ones with their advantages and disadvantages over classic techniques.

One technique that was recently introduced for studies on muscles is the elastography [56, 57]. Elastography is mainly used for the estimation of muscle forces and it is an imaging technique that visualize the stiffness properties of tissues. During elastography a perturbation of the tissue is created, the response is observed and the resulting information are processed. The response is usually observed either with MRI or ultrasounds. For studies on muscles, a perturbation with a shear wave is applied to the muscle and the the velocity of propagation of the wave is observed. The speed of the wave changes with the stiffness of the tissue, giving information on the instantaneous state of the muscles. The stiffness of the muscle can be charac-

terized with the muscle shear modulus, a mechanical property of the muscle tissue. Additionally muscle shear modulus was demonstrated to have a linear relationship to both active and passive muscle force. It showed important advantages over the EMG, such as the fact that the method is not influenced by muscle fatigue and the fact that force estimation methods using EMG do not consider passive forces [56]. However it presents limitations as well, in fact it is unclear how it would behave in areas where there is a high density of muscles. Furthermore it requires the use of an ultrasound machine and a mechanical vibrator, which makes the setup not easy to apply.

Another technique that was utilized is electric impedance myography (EIM). It is a non invasive technique that consists in the application and measurement of high-frequency, low intensity electrical currents [11]. A current generator is placed on the skin in the form of an anode and a cathode placed in the opposite sides of the forearm. Electrodes for sensing and for reference are placed on the forearm as well. When the muscle activates the amplitude of the measured currents change and the quantification of the change allows to discriminate between different tasks. The method has the advantage of being able to consider the effect of the deep muscles for a better discrimination of their effects and role. However it does not allow the differentiation of the action of each of the single muscles in the section but it rather provides an index for the identification of the task useful for example for a classification.

Other methods worth citing are EMG-CT [58] and works using discrete models [59] where the effect of signal propagation is studied with the use of finite elements to model the volume conductor. Even though the results provided are interesting, the complexity that derives from the construction of the model using finite or boundary

elements hinder the use of these methods for bigger studies.

2.5 Neuromuscular electrical stimulation

Electrical stimulation (ES) is a technique that elicit contraction of muscles through the application of an external current impulses. An important distinction can be found when applying external current impulses to muscles. In particular when the current impulses are producing a depolarization of the muscle without directly providing function the ES is called neuromuscular ES (NMES). When the electrical current is instead, directly enabling a functional movement it goes under the name of functional ES (FES)[60].

NMES is a technique that found multiple applications even outside the clinical field. It can be used as training tool for athletes to strengthen particular muscle groups, it can be used as rehabilitation tool for patients with partial or total motor dysfunction , it can be used as diagnostic tool to evaluate the muscle functionality[60, 61].

The motor units activated by a current depends on a combination of factors that included motor axon diameter and the location of the axon and its branches relative to the stimulating electrodes[28]. As a consequence, electrical stimulation with small pulses activates motor units in a random order and not in the order of increasing motor unit size as occurs during voluntary contraction. However, when stimulation is provided with longer pulses (1ms), it causes the selective activation of particular type of fibers that generate a recruitment order more similar to that observed during voluntary contractions.

The maximal excitation is obtained when the electrodes through which the currents is applied are placed over the motor point of a muscle. When this happens, the motor axons fires action potentials that cause the starting of action potentials on the innervated motor units. For this reason, before an NMES session the motor points needs to be identified. This is usually done with a scanning or surfing procedure where the operator fix the anode to the nerve trunk and moved the catode over the approximate area of the motor point in order to find the point where the current cause the strongest visible contraction.

FES is an attractive technique in the field of neuromuscular rehabilitation and many studies were attempted, aiming to provide people with neuromuscular impairment a way to regain control of wither upper or lower limbs. It bypasses the damaged neurological segment, applying a pattern of currents to muscles that can trigger a controlled contractions. FES may require sophisticated circuitry with multiple channels and the design of appropriate triggering mechanisms [60]. Muscles are stimulated applying transcutaneal currents from a matrix of electrodes on the skin surface. A drawback of this approach is that, to overcome the high resistance of the skin, high voltages are required. Furthermore this superficial FES usually stimulates only superficial muscles, while deep muscles are left unused.

One alternative FES approach was proposed by Loeb et al. [62] where they injected biocompatible microstimulator inside all muscles in the paralyzed body segment. These microstimulators are controlled wireless from outisde with an external device that can provide different stimulation patterns. They found some application in clinical field including rehabilitation of hypotrophic muscles and stimulation of peripheral nerves [63], but still many difficulties persists for a broader application

for limb rehabilitation.

2.6 Electrical Network Analysis with Graph Theory

One of the main assumption in this thesis is that the interaction between the morphological parts of the forearm section obtained from an MRI are analogous to that of a electric network. In particular, the assumption made is that it is possible to lump the activity of all the elements in the scanned image using elements of an electrical network and therefore it is possible to solve the network using concepts of circuit theory.

Circuit theory is usually used to study electrical phenomena that are happening in an electrical network i.e. in a medium where the electrical effects are constrained to a defined path [64]. The medium is described with elements that abstract the characteristic of the surrounding material. These elements can be resistances, inductance or capacitance and are interconnected with each other. The electrical quantities evaluated on a circuit are voltages and currents, which are evaluated at the extremes of the elements. The closed network made with the interconnections of all the element describing the medium is called electrical circuit and describes how the electrical energy is distributed, stored or dissipated inside the system.

The energy is flowing in the circuit as charges and voltage and current are variables that describes its distribution. A flow of charge is described with a current while the energy needed to let charges flow is described with voltage. Voltage and

current define the energy and power flow in the system. Electric power through an element P_E of the circuit is defines as

$$P_E = V \cdot I \quad (2.1)$$

where I is the current flowing through the element and V is the voltage at the terminal of the element. The sign of the power gives information on the action of the element. A positive power indicate that the element is dissipating energy, while a negative power indicates that the element is absorbing power.

The behavior of the circuit depends on the nature of the elements that compose it. Each type of element describe the relationship between the currents and the voltage through a constitutive equation. The main elements are resistors, capacity and inductors. Resistors are linear elements while capacitors and inductors are non-linear elements. Since the electric networks described in the next chapters will solely include linear elements, the following description will limit to resistors.

Resistors are elements that resists the flow of charge. The constitutive equation of a resistor linearly relate the voltage and the currents, and is also known as as Ohm law :

$$V = R \cdot I \quad (2.2)$$

where R is called resistance and it a property that define a resistor. The inverse of the resistance $G = \frac{1}{R}$ is called conductivity. The higher the resistance, i.e. the lower the conductivity, the more the element opposes to the charge flow. Conversely, the lower the resistance, i.e. the higher the conductivity, the less the element opposes

to the current.

When interconnecting to form a circuit, the points where two or more elements connect are called nodes. While the constitutive equations of each elements describe its behavior to the passage of a current, how the elements are connected to each other in the circuit is described with the Kirchhoff's laws. The Kirchhoff's laws derive from the conservation of energy and charge principles.

The Kirchhoff law of current (KCL) states that the algebraic sum of the currents at each nodes is zero:

$$\sum_{k \in K} i_k = 0 \quad (2.3)$$

where i_k are all the currents at the node K .

The Kirchhoff law of voltage (KVL) states that the sum around any loop (i.e. closed path in the circuit) is zero:

$$\sum_{l \in L} v_l = 0 \quad (2.4)$$

Resistors in the network can be arranged in series or in parallel, depending on how their terminals are connected (Figure 2-7).

A set of resistors are in series when the end terminal of one resistor is the starting terminal of the next resistors. In a series of resistors the current flowing through each element is the same. Conversely, a set of resistors are in parallel when they all share both the terminals. As a consequence the voltage between the terminals is the same for all the resistors.

Series and parallel resistors can be described with an equivalent element describ-

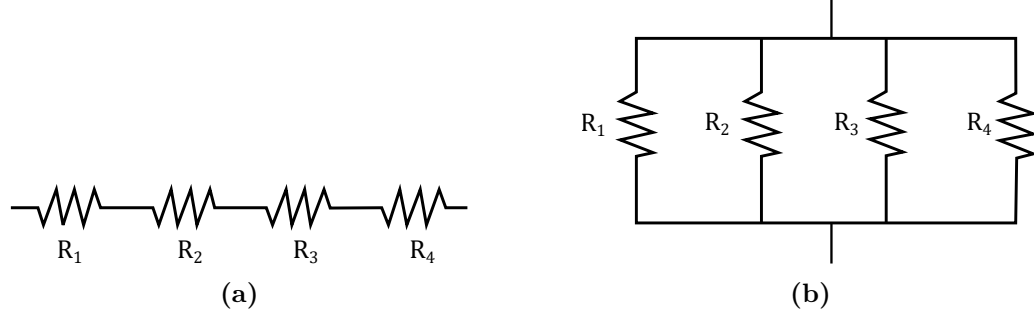


Figure 2-7: Resistors possible settings. (a) series of resistors and (b) resistors in parallel

ing the behavior of the set of resistors. In particular a series of P resistors can be described with a single equivalent resistor R_{eq} whose resistance is

$$R_{eq} = \sum_{p=1}^P R_p. \quad (2.5)$$

Since the voltage across a series of resistors is divided according to the value of each of the resistance in the series, a series of resistors acts as a voltage divider^{??}. A parallel of T resistors can be instead described with another single equivalent resistor R_{eq} whose resistance is

$$\frac{1}{R_{eq}} = \sum_{t=1}^T \frac{1}{R_t}. \quad (2.6)$$

Since the currents at the common node, split between the different resistances, the parallel of resistors acts as a current divider.

The idea under the method presented in this thesis, is that a section of the forearm can be assumed to behave like a power grid, where the muscles are the generators and the electrodes are points in the grid where it is possible to read the voltage. In

order to find the values of the variables in the grid, i.e. voltage and current, a circuit analysis needs to be performed. To analyze a circuit means to calculate the value of current and voltage for each of the elements in the circuit. Since each element has 2 unknown, even for small circuits, the number of equations that needs to be considered can be considerably large. One convenient way to analyze a circuit, that has been used since the very beginning of circuit theory, is with the use of algebraic graph theory. A graph is a mathematical structure that can be used to describe a topology using nodes and edges. Nodes are abstract objects that can assume different meaning, while edges are connections between a pair of nodes and are uniquely identified by that pair. The elements of an electric network and the way they interconnect can be therefore described as a graph where the nodes are corresponding to the nodes of the network and the edges represent the elements.

Usually an electric circuit is modeled with an undirected (i.e. with undirected edges) graph G of n nodes and e edges with an additional node 0 to model the common ground and n additional edges to model the connection of each of the nodes to the ground. An arbitrary orientation of the edges can be introduced, and for each of the oriented edges (i, j) , with edges connecting with the common ground oriented as $(i, 0)$, i.e. the edge is directed from the common ground to the node. When an orientation is assigned, it is possible to describe the graph not including the ground node with an incidence matrix $B \in \mathcal{R}^{n \times e}$ defined as:

$$B_{ie} = \begin{cases} +1 & \text{if the edge } e \text{ is } (i, j) \text{ for some } j \\ -1 & \text{if the edge } e \text{ is } (j, i) \text{ for some } j \\ 0 & \text{otherwise.} \end{cases} \quad (2.7)$$

It is easy to verify that $\mathbb{1}_n^T B = \mathbb{0}_e^T$, where $\mathbb{1}_n \in \mathcal{R}^n$ is a vector of ones and $\mathbb{0}_n \in \mathcal{R}^n$ is a vector of zeros. When considering the ground node, the incidence matrix is updated as follows:

$$B_{ground} = \left[\begin{array}{c|c} -\mathbb{1}_n^T & \mathbb{0}_e^T \\ \hline \mathcal{I}_n & B \end{array} \right] \quad (2.8)$$

where $\mathcal{I}_n \in \mathcal{R}^{n \times n}$ is the identity matrix.

For each of the directed edges it is possible to define[65]:

- an oriented current flow $f_{i,j} \in \mathcal{R}$
- an oriented voltage difference $u_{i,j} \in \mathcal{R}$

Given these variables defined for each of the edge in the graph, the duality allow the use of graph properties to have a matrix description of the Kirchoff laws. For convenience it is usual to define 2 additional variables for each of the node i :

- A current $I_i = -f_{i0}$ indicating the current flow from the ground node, also called external current
- A potential V_i for all the nodes plus the ground. The potentials are referred to a arbitrary reference that is set to be the ground potential which is set to be zero $V_0 = 0$.

Once set these auxiliary variables, KCL and KVL can be rewritten in a simple way. In fact using this notation, KCL can be rewritten

$$I = Bf \quad (2.9)$$

KVL can be rewritten in a simple way. Assuming $V_0 = 0$ in fact:

$$u = B^T V \quad (2.10)$$

meaning that each of the voltage drop u_{ij} is calculated as difference between the potentials $V_i - V_j$ with the sign convention given by the values in the incidence matrix B .

The combination of KCL and KCV provide a set of $n + e$ equations in for the $2n + 2e$ unknown (V, u, I, f) . The remaining equations are given by the constitutive equations of the elements on the edges. For resistive elements the constitutive equation is simply the Ohm law described before :

$$u_{ij} = r_{ij} f_{ij} \quad (2.11)$$

where $r_{ij} > 0$ is the resistance of the edge (i, j) . These set of equations allow to solve the circuit exploiting the properties of the graphs.

2.7 Conclusions of this chapter

In this chapter an overall introduction of the topic treated in this thesis was presented. How the control signal is generated and and flows from the primary cortex to the

target muscles was briefly explained. The processes through which the contraction happens was described along with the dynamic characteristics of the muscles. The inherent problem of the redundancy in the musculoskeletal system was explained and the current hypothesis on how this redundancy is solved by the CNS were briefly presented.

The main methods for the investigation of the muscular activity at different level, i.e. EMG and MRI were described with a focus on the use of high-density EMG and muscle functional MRI in relation to studies aiming to give a quantification of the muscle activation. The limitation of the current approaches for the estimation of muscle activation pattern of all the muscles on densely populated anatomical segments were described, providing a set of requirements for the method that will be described later on.

Finally a short description of the EMS and the circuit theory and circuit analysis was provided as a reference for their usage in the next chapters.

This chapter wanted to give a brief, yet complete description to the reader of all the processes that happen from the motor intention to the actual muscular contraction, along with the main methodologies to investigate motor phenomena. It is important to underline that the motor control presents further additional complexities that were not presented in this chapter. Interested readers are referred to specialized literature on the topic.

In the next chapter I will introduce a method for the estimation of the activation pattern of muscles on the forearm from the EMG exploiting the MRI information to create a subjective resistive model of one section of the forearm.

Chapter 3

A method for the estimation of muscles activation

In this chapter the proposed method for the estimation of muscles activation is firstly introduced, along with details about the rules used to translate the information on the MRI into an electrical network model. The estimation methods and the assumption on which it is based are described as well.

The model presented was applied on isometric wrist and finger movements on a 4 participants sample and the results are presented. A validation based on anatomical information from specialized literature and based on the fitting with the measured EMG of the estimated currents re-projected on the electrodes' space are utilized [1, 4, 5]. In the last part of the chapter an alternative validation method for the model matrix with the use of electrical stimulation is presented.

3.1 Experimental Procedure

An experiment involving 4 healthy participant (2 males, 2 female, average age : 27.3 ± 2.3 years old) was set for this study. All participants gave an informed consent to take part to the study. The experimental protocol was approved by the ethics committee of the University of Tokyo. None of the subjects had any reported neurological or muscular history at the time of the experiment.

For the experiment the participants had to perform simple motor task at the wrist and the metacarpal joint of index and middle finger while HD-sEMG was acquired on their forearm. Prior to the motor task experiment, each participant underwent an MRI scan of the forearm utilized during the motor task.

3.1.1 MRI acquisition

For each participant a T1-weighted image of the forearm was acquired. The scan was recorded with a 3T Siemens Verio (Siemens Healthcare GmbH, Erlangen, Germany) scanner at the National Center of Neurology and Psychiatry (Kodaira, Tokyo, Japan) with the following parameters setting:

- **Voxel Resolution :** $0.2 \times 0.2 \times 3 \text{ mm}$
- **Matrix Dimension :** $448 \times 448 \text{ pixel}$
- **Repetition Time :** 11 ms
- **Echo Time :** 4.92 ms

The forearm was held in supinated position with the hand palm facing upward for consistency with the set up during the HD-sEMG acquisition.

A set of liquid Vitamin E capsules were taped on anatomical reference points of the wrist and of the elbow for subsequent registration purposes. Since vitamin E is fat soluble, the marker capsules contained a high amount of fat which shows a higher contrast on T1-weighted scan and were therefore easily identifiable. Markers were put on the humerus lateral and medial epicondyle, radial styloid, ulnar head and ulnar olecranon.

3.1.2 HD-sEMG acquisition

For the electromyographic signal acquisition custom design high density electromyographic sheets were used. Two different size of electrodes sheet were designed to accommodate the different forearm size: a shorter sheet of $195 \times 52 \text{ mm}$ with $10 \times 19.5 \text{ mm}$ inter-electrode spacing and a longer sheet of $270 \times 52 \text{ mm}$ with $15 \times 19.5 \text{ mm}$ inter-electrode spacing. Both size of electrodes sheet contained 64 electrodes arranged in a 16×4 electrodes. Before being attached to the skin a layer of thin foam with adhesive on both sides was stuck to each electrodes sheet. The foam layer had holes in correspondence of the electrodes position that were filled with conductive cream. Each participant had the forearm covered with 4 electrodes sheets wrapped transversely. For the purpose of this study only a single row was considered. Additional Ag/AgCl adhesive electrodes (Ambu, Ballerup, Denmark) were stuck to the radial styloid and the metacarpophalangeal joint of the thumb on the same arm as, respectively, electrical ground and reference (Figure 3-1 *Left*).

The signal was amplified and acquired with a RHD2000 Evaluation System (Intan

Technologies, Los Angeles, CA, USA) at a sampling frequency of 2500 Hz with no prior analog filtering. The signal was bandpass filtered offline on Matlab (Mathworks, Natick, MA, USA) with a 4th order Butterworth filter between 20 and 450 Hz to remove motion artifacts, power noise and high frequency noise.

The position of the electrodes and the anatomical references marked during the MRI were collected with a Polhemus Fastrak 3D digitizer system (Polhemus, Colchester, VT, USA) for subsequent registration. After acquiring the position of the markers and of the electrodes, the electrode sheets were further wrapped with a sport elastic bandage to maximize the adhesion between the electrodes and the skin.

The full experimental setup is depicted in Figure 3-1. The subject lay supine on

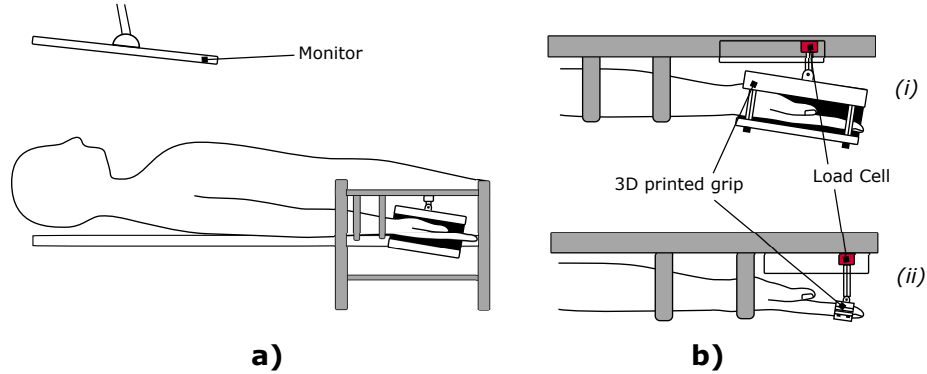


Figure 3-1: Experimental Setup. *Left* : Top and bottom view of electrodes positioning on the forearm. Four sheets of 64 electrodes were wrapped around the forearm in order to cover the maximum amount of its surface. A reference electrode was positioned on the metacarpophalangeal joint of the thumb. A ground electrode was stuck to the radial styloid. *Right*: (a) Position of the subject during data acquisition. The subject was lying down facing a monitor through which a visual feedback was given of the applied force. The forearm was held in supine position, with the hand palm facing upward; (b) Force measuring structure for wrist movements (i) and for finger tasks (ii). The hand/finger was enclosed in a custom 3D printed structured coupled with a load cell to measure the force amplitude.

a sofa. A real time visual feedback of the exerted force was given with a monitor mounted over the subject's face. The right forearm of the subject was then positioned on a custom made alloy frame that sustained the forearm and the hand horizontally, parallel to the floor. The wrist was held in supinated position, with the face palm facing upwards, in order to avoid crossing between the ulna and the radius bones. The hand was inserted in a 3D printed cage coupled to the alloy frame through a force sensor in palmar position and a sensor in lateral position, able to measure, respectively, exerted forces along vertical and lateral direction. A different setup to constrain the hand was used to measure force during finger tasks. In particular the target finger was put into a 3D printed structure connected to a force sensor that measured the force exerted along the direction normal to the surface of the electrode (Figure 3-1.b). Forces were measured with an Arduino board at a sampling frequency of 10 Hz.

Each participant was asked to perform five different isometric task at two different force levels, 25% and 50% of maximum voluntary contraction (MVC) force based on the visual feedback given through the monitor. Prior to each of the task each participant was asked to perform a single MVC contraction to calibrate the force feedback. The isometric tasks that were executed were :

1. Middle finger metacarpophalangeal(MCP) joint extension
2. Wrist flexion
3. Wrist extension
4. Ulnar deviation

5. Index Finger MCP extension

each of which was repeated 15 times. Each repetition consisted of a 2s force raising, 5s force holding, 2s force release followed by 15s of rest. In order to avoid effects related to fatigue and adaptation the first and the last 2 repetition were ignored in the analysis. Therefore all the results are related to the central 11 tasks.

3.2 Methodology

We propose a method that allows the estimation of the muscle activation pattern from a selected MRI slice and the EMG signals collected from electrodes around the selected section. The conductive volume and the interaction between the different tissues is described with a lumped parameter model that is described with a graph. The method solve an inverse problem for the identification and the quantification of the activity of muscles involved. The conductive properties are described with a resistive network connecting the electrodes and different tissue elements represented in the selected MRI slice. The MRI slice is chosen in order to include the muscles responsible for the movements targeted in the study.

Muscles are localized on the MRI slice with a segmentation step, while electrodes are identified with a registration step. Muscles and electrodes are the nodes of a graph which edges are defined based on the anatomy observable from the MRI slice. The model is then solved assuming the muscles as current generators placed on muscle nodes to obtain an estimation of muscles activity. The model construction process can be separated into three main sections which will be explained in detail within the next subsections:

- Morphological information segmentation and registration
- Electric Network Construction
- Muscles Current Pattern Estimation.

An overall structure of the method is depicted in figure 3-2.

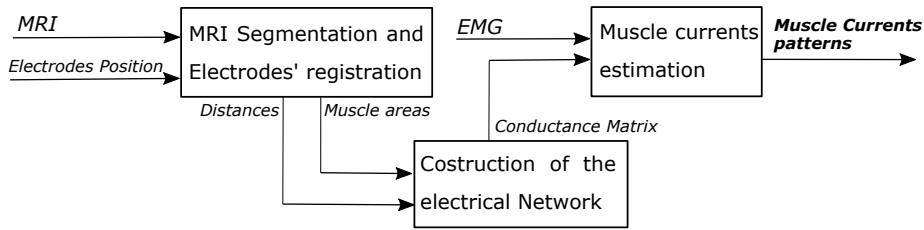


Figure 3-2: Diagram of the proposed approach. Three main parts can be identified, *MRI segmentation and electrodes' registration*, *Costruction of the electrode network* and *muscle currents estimation*. From the left, the MRI segmentation and electrodes' registration block processes the information of the MRI slice and the electrodes' position to estimate the distance between the elements (muscles and electrodes) in the MRI and the muscles' cross section areas. This information is then used to create and weight the edges of a graph describing the interaction between the nodes representing muscles and electrodes. In the *Muscle currents estimation* block, the EMG is exploited to obtain an estimation of the muscle activation patterns through the solution of an inverse problem using a conductance matrix describing the topology of the graph and of the related electrical network.

3.2.1 Morphological information segmentation and registration

All the different anatomical structures (e.g. tissues, bones) visualized in the MRI slice can be discriminated and identified through a segmentation process. Segmentation is an imaging processing technique through which the different anatomical structures

are identified on a diagnostic image. In the forearm it is possible to mainly identify four types of tissues: bone, skin, fat, and muscular tissue. While the skin, fat and bones can be easily identified due to their different contrast in the T1-weighted MRI image, each of the different muscle needs to be properly identified and outlined.

The forearm contains about 20 muscles which are responsible to control the degrees of freedom of forearm and wrist and some of the movements at fingers level. In particular, forearm pronation/supination, wrist radial/ulnar deviation, wrist flexion/extension and finger flexion/extension can be controlled using forearm's muscles. It is possible to roughly divide the forearm's muscles into two groups based on their function: extensors along the posterior side and flexors on the anterior side. Additionally, extensor and flexors can be further subdivided into superficial and deep muscles. Muscles delineate complex paths along the forearm. MRI slices considered at different longitudinal coordinate along the forearm can therefore depict different muscle sets. The segmentation process allows the identification and definition of position, cross sectional areas, and boundaries of each of the muscles in the MRI slice (Figure 3-3).

For each participant one MRI slice was selected. All the slices were segmented and processed with imaging software ImageJ [66]. The selected slice contains for every subject the same set of muscles. . The considered set of muscles was the following: Abductor Pollicis Longus (APL), Extensor Pollicis Longus (EPL), Brachioradialis (BR), Extensor Digitorum (ED), Extensor Carpi Radialis Longus (ECRL), Extensor Carpi Radialis Brevis (ECRB), Extensor Carpi Ulnaris (ECU), Extensor Digiti Minimi (EDM), Flexor Digitorum Profundis (FDP), Flexor Digitorum Superficialis (FDS), Flexor Carpi Ulnaris (FCU), Flexor Carpi Radialis (FCR).

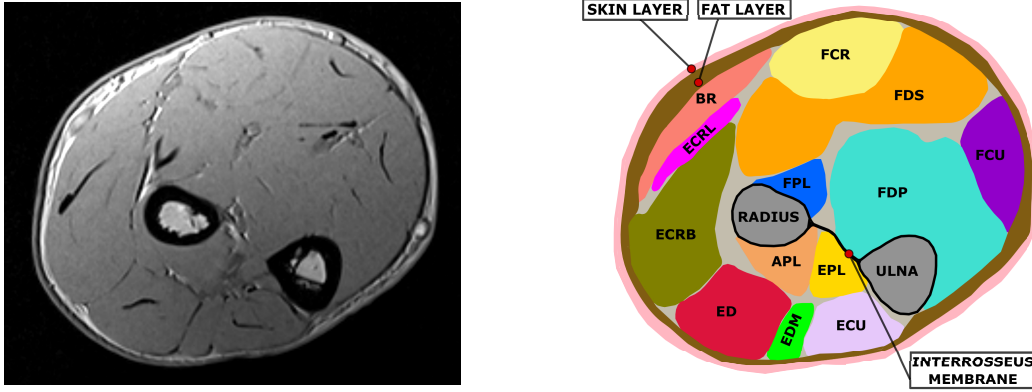


Figure 3-3: Example of segmentation on an MRI slice. On the left the original MRI is depicted, on the right its segmentation is reported. Muscles are represented with different colors, the radius and ulna bones are reported in gray. It is possible to observe the interosseus membrane connecting ulna and radius and dividing the posterior and the anterior side muscles. Skin and fat layers are colored respectively in pink and brown.

The skin layer has been ignored for the purpose of this work and its thickness has been included into fat layer thickness. Fat layer thickness is estimated as the average value of electrode-muscle distance along the arm circumference.

The electrodes' coordinates and the MRI scans had a different reference frames, since they were measured in different moments with different devices. In order to correctly locate the position of the electrodes on the volume of interest of the MRI, a registration step was performed prior to the creation of the model. A registration is a procedure to estimate the optimal transformation that match the coordinate system of the electrodes to the coordinate system of the MRI. The registration was done using 3D slicer [67, 68], minimizing the distance between the position of the anatomical markers on the MRI and the position of the markers acquired with the digitizer. The electrodes around the arm that were closest to the chosen slice were selected and their 2D projection on the MRI section was calculated (Figure 3-4a).

The position of the electrodes on the slice was set to be the closest point identified on the skin of the 2D projection of the electrodes (Figure 3-4b). The mean and the maximum distance error made during electrodes' projections steps are reported in Table 3.1 for all subjects. On the upper rows the errors for the projection on the selected slice are reported while on lower rows the errors on the projection on the skin surface are reported. On average the error during the projection on the selected slice is between 3 and 4.2 mm, with maximum values ranging from 7.5 to 11 mm. The distance errors on the projection on the skin surface was lower, with an average error smaller than 1 mm for all subjects and maximum values going from 1.5 to 3 mm.

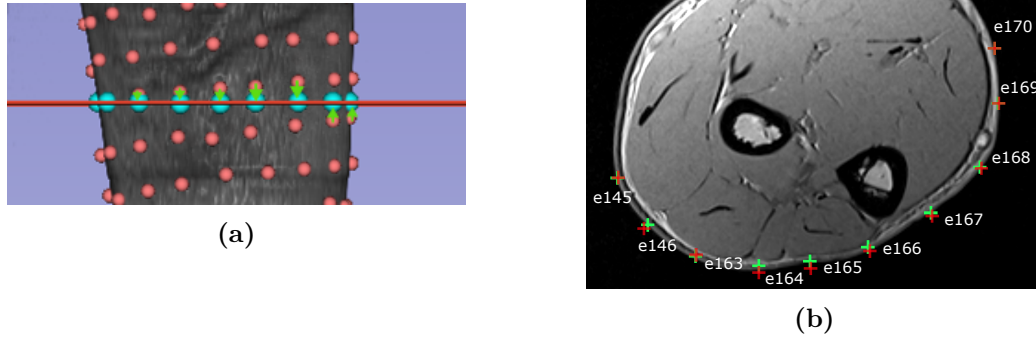


Figure 3-4: (a) The projection of the electrodes closest to the selected slice plane. The real electrodes position is indicated with a red sphere, the MRI plane is indicated with a red line and the projected position is indicated with a light blue sphere. The projection is depicted with a green arrow. (b) Section of the MRI with the position and the number of the electrodes. The projection of the electrode 3D position on the 2D slice is represented with a red cross. Such points are further projected on the skin (green cross) to find the closest position on the forearm surface.

Once muscles and electrodes are correctly positioned and identified on the MRI

Table 3.1: Distance errors in the projection of the electrodes' positions from the 3D space to the skin on the selected MRI slice. The distance errors in the projection on the selected slice as shown in Figure 3-4a are reported on first two rows of the table. The distance errors for the projection of the position on the skin surface as shown in Figure 3-4b are reported on the bottom two rows. For each of the subjects, the mean and the maximum distance errors are reported.

		<i>Subject 1</i>	<i>Subject 2</i>	<i>Subject 3</i>	<i>Subject 4</i>
<i>On the slice</i>	Mean distance [mm]	4.121	3.848	3.167	3.540
	Max distance [mm]	11.829	9.029	8.818	7.521
<i>On the skin</i>	Mean distance [mm]	0.890	0.862	0.789	0.620
	Max distance [mm]	2.217	1.980	3.085	1.570

slice plane, it is possible to measure distances between muscles and electrodes. In particular, it is possible to identify three type of distance:

- electrode-electrode (e-e) distance
- muscle- electrode (m-e) distance
- muscle-muscle (m-m) distance

Distances have been calculated from the centroid of the segmented cross sectional area for muscles. Electrodes' distances were calculated from the projection of the electrode position on the skin. In an MRI slice it is possible to identify n_m muscles and n_e electrodes on the skin surface.

3.2.2 Electric Network Construction

The anatomical information represented in the results of the segmentation can be described with a topology. A topology can be used define the connections between

the different elements identified in the segmentation. One common way to describe a topology are graphs, mathematical discrete structures constructed with a set of nodes and a set of edges. A node represent an object of the structure that holds a meaning that depends on the application. Edges describe a relationship between a pair of nodes.

To describe the anatomical information contained in the MRI slice it is possible to model muscles and electrodes as nodes of a graph, with edges that describe connections that are defined with a set of custom rules based on several assumptions and prior anatomical information. The rules used in this work are listed as follows:

1. Each electrode defines a sector of the forearm section bounded by two lines going from the centroid of the forearm cross-section to the two adjacent electrodes(Figure 3-5).
2. All muscles included in a sector with a fraction of their area greater than 5% of their cross sectional area are connected to the electrode that defines that sector.
3. If between the fraction of the muscle in a sector and the electrode defining that sector there is a structure hindering the electric flow interposed (e.g. bones, connective tissue), that edge is not considered.
4. In general a muscle node is connected to another muscle node only if they are adjacent on the segmented image. Exception are considered to take into account specific anatomical structure that are known to alter the currents flow in the volume. In particular the effect of the interosseus membrane between

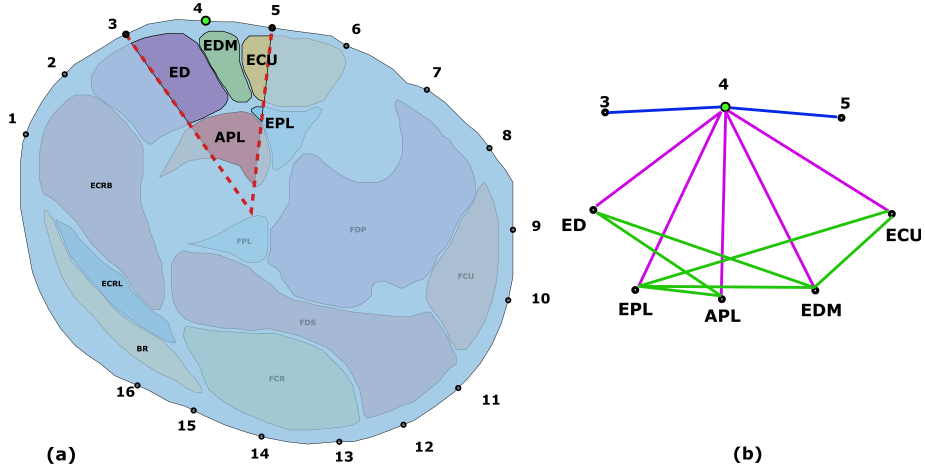


Figure 3-5: Example of one step of the graph creation. (a) Sector belonging to one of the electrodes, indicated with a green dot. The muscles that are included (ED, EDM, ECU, APL, and EPL) are highlighted with the area that is accounted for. (b) Graph created from the section considered in (a). e-e edges are indicated in blue, e-m edges are indicated in purple and m-m edges are indicated with green lines.

the ulna and the radius has been considered.

5. The fat layer is assumed to be of constant thickness around the section circumference. Such thickness is set to be the average obtained from the segmentation and it includes the skin thickness.
6. Since it is an electrical network and additional node has to be added to consider the grounding.

This set of rules allows the definition of a graph with N nodes and E edges that specifically describes the anatomy of the subject and the electrodes setup for a specific cross section of the forearm. Each edge is weighted based on the nature of the nodes pair (n_1, n_2) that defines it. The weight is set to be the electric conductivity

G_{n_1, n_2} between the nodes pair (n_1, n_2) obtained as

$$G_{n_1, n_2} = g \cdot r(n_1, n_2) \quad (3.1)$$

where g is the conductance of the tissue interposed between the 2 nodes and $r(n_1, n_2)$ is the distance between the nodes n_1 and n_2 . The conductance for the considered tissues (i.e. muscle, fat and skin) are those reported by Lowery et al. in [69]: $g_{skin} = 4.3 \cdot 10^{-1} S/m$ for the skin, $g_{fat} = 0.04 S/m$ for the fat and $g_{muscle} = 0.09 S/m$ for muscle along the transverse direction.

The nature of the node pair in the edges define the type of conductance that is chosen. As described for the measured distance, it is possible to identify electrode-electrode(e-e), muscle-muscle(m-m) and electrode-muscle(e-m) type of edges. For (e-e) and (m-m) edges, the weight can be assigned using Equation (3.1), assuming that the current between two adjacent electrodes flow through the skin and that the current between two muscles flow through only muscle tissue. In particular the conductance for (e-e) edges G_{ee} and (m-m) edges G_{mm} can be calculated as

$$\begin{aligned} G_{ee} &= g_{skin} \cdot d_{ee} \\ G_{mm} &= g_{muscle} \cdot d_{mm}. \end{aligned} \quad (3.2)$$

In the case of (e-m) edges the conductance value G_{em} to weight the edge was calculated as the series of two resistive elements in order to consider that current flow from muscle to electrode passing through muscle and fat tissue

$$G_{em} = \frac{G_{fat} \cdot g_{muscle}(d_{em} - D_{fat})}{G_{fat} + g_{muscle}(d_{em} - D_{fat})}. \quad (3.3)$$

To consider the effect of partial inclusion in the sector, the conductance of the (e-m) edges were weighted with the normalized area

$$\hat{G}_{em} = G_{em} * \left(\frac{A_{em}}{A_m} \right) \quad (3.4)$$

where A_{em} indicates the area of the muscle m included in the sector defined by the electrode e , and A_m is the total area of the muscle m .

Each of the muscle nodes was considered as a current generator to model the active muscle behavior. Finally, all the nodes were connected to the ground node with a shunt resistance. The shunt resistance has been set to $D_{skin} \cdot G_{el-el}$ and $D_{muscle-bone} \cdot G_{muscle}$, respectively for electrode nodes and muscle nodes, where D_{skin} is the average distance between electrodes and $D_{muscle-bone}$ is the average distance between the centroid of muscles and the closest bone (ulna or tibia).

The resulting electrical model can be described exploiting the principles of graph theory. Under the assumption of no external power injection and in static condition the current of the nodes can be described with the following relationship [65]:

$$\mathbf{I} = (\mathcal{L}_R + \mathbf{G})\mathbf{V} \quad (3.5)$$

where $\mathbf{I} \in \mathbb{R}^{N \times 1}$ is the vector of currents, $\mathbf{V} \in \mathbb{R}^{N \times 1}$ is the vector of node potentials, $\mathcal{L}_R \in \mathbb{R}^{N \times N}$ is the conductance matrix and $\mathbf{G} \in \mathbb{R}^{N \times N}$ is the shunt conductance matrix. If \mathbf{G} has at least one non-negative element, equation 3.5 can be inverted to obtain the voltages on the nodes

$$\mathbf{V} = (\mathcal{L}_R + \mathbf{G})^{-1} \mathbf{I} = \mathbf{F} \mathbf{I} \quad (3.6)$$

where $\mathbf{F} = (\mathcal{L}_R + \mathbf{G})^{-1}$ is the matrix describing the system. With equation 3.6 it is possible to estimate the potential of the nodes with respect to the reference value, which is usually set to $V_0 = 0V$.

3.2.3 Muscles Current Pattern Estimation

Using the built model, the muscle activities are estimated solving an inverse problem. Equation 3.6 and 3.5 describe the linear relationship that relate the currents and the voltages in the network. Equation 3.5 describes the relationship between the potentials and the currents on the node. Since we are only interested in how the muscles' current are reflected on the electrodes potentials it is possible to simplify the problem reducing the dimension of the system matrix, i.e. selecting the row corresponding to electrodes nodes and columns corresponding to muscle nodes from the matrix F . The resulting matrix is a matrix $\tilde{\mathbf{F}} \in \mathbb{R}^{n_e \times n_m}$ where the i^{th} column is the potential that would be present on the n_e electrodes if the i^{th} muscle is activated with unitary current.

With this notation it is possible to describe the transformation from muscles currents to electrodes' potentials as follows

$$\mathbf{V}_e = \tilde{\mathbf{F}} \mathbf{I}_m \quad (3.7)$$

where \mathbf{V}_e is the $n_e \times 1$ electrode potential vector and \mathbf{I}_m is the $n_m \times 1$ muscle current vector.

Since the number of electrodes is always higher than the number of muscles, the problem is over-determined. A minimum norm approach would therefore lead

to unstable solutions. To find a unique solution, a regularization is needed. We assumed that the voltage measured at the sEMG is caused mainly by the activities of big muscles, therefore the regularization is penalizing the activation of muscles with small cross sectional area. The resulting estimated muscles current $\hat{\mathbf{I}}_{\mathbf{m}}$ has been therefore calculated as follows:

$$\hat{\mathbf{I}}_{\mathbf{m}} = \tilde{\mathbf{F}}^T (\tilde{\mathbf{F}} \tilde{\mathbf{F}}^T + \lambda \mathbf{I})^{-1} \mathbf{V}_{\mathbf{e}} \quad (3.8)$$

where λ is a regularization vector that has been set to the inverse of the cross sectional area of all the muscles.

3.2.4 Validation Criteria

A direct evaluation of forearm's muscle activity would entail the use of invasive probe directly inserted on each of the considered muscles. This is practically impossible because of the pain and the discomfort that it would cause to the person. Furthermore it would only allow to record local activity of the fibers and not an overall activation of the muscle. Therefore, to validate the results indirect methods must be used.

In this work we considered two criteria, one qualitatively based on functional prior knowledge and the other quantitatively measuring the fitting on the measured sEMG data on the electrodes' space. To qualitatively evaluate the results from an anatomical point of view, the muscles involved in the examined motor task has been compared to those reported in the literature. In particular the muscles involved in each of the movements are the following:

- Middle finger extension : **ED**, EDM

- Wrist flexion : **FCU**, **FCR**, APL, EDM
- Wrist extension: **ECU**, ECRL, ECRB, ED
- Ulnar deviation: **FCU**, **ECU**, FCR, ECR,

where the muscle highlighted with a bold font are considered the main responsible for the movement.

The method was evaluated comparing the estimated active muscles with those reported as main responsible by specialized literature[70, 71]. A quantitative performance evaluation of the method is conducted comparing the projection of the estimated muscle on the electrode space with the measured sEMG using the Goodness of Fit(GOF) index. This gives a quantitative value of the amount of the sEMG information that is explained by the estimated activity. The GOF is evaluated using the Normalized Root Mean Square Error (NRMSE) as follows:

$$GOF = 1 - NRMSE = \frac{RMSE}{max - min}. \quad (3.9)$$

With this definition, a value of GOF close to 1 indicates a higher fitting on the experimental sEMG data, with 1 meaning a perfect fit. Conversely, lower values of GOF indicates lower fitting performance.

3.3 Results

The results of the segmentation and registration process are represented in Figure 3-6. Each muscle is represented with a different color and the projection of the electrodes

on the skin is represented with a dot and a number indicating the sequential order of the electrodes.

The RMS profile of the sEMG for the studied isometric tasks at 50% of the MVC are depicted with polar plots in Figure 3-7. Each task is shown with different line color. For the sake of clarity the polar plots were created assuming that the arm section is circular and that it is divided into $n_e + 1$ sectors by n_e electrodes arranged with equal space between each other. The value of the RMS voltage is represented with a circle on the line. Each subject has a different number of electrodes depending on the size of the forearm. To better identify the position of the electrodes, the portion of the cross section area with extensor muscles (posterior side) and flexor muscles (anterior side) are depicted with a different background color on the section, respectively with in red and green.

The first two subjects have similar RMS values with similar RMS sEMG profiles along the circumference, while subject 3 and 4 have a higher RMS value for the middle finger extension. For each of the tasks it is possible to observe a subjective sEMG profile around the arm.

The results of the current estimation procedure and the relative voltages reprojected on the electrodes' space are reported in Figure 3-8 and in Figure 3-9 for tasks at 25% MVC and 50% MVC, respectively. For each subject and given task, the top graph represents the estimated currents generated by each of the muscle node, while the lower graph represents the reprojected voltage on the electrode space compared to the measured sEMG. The bar on the top graph represents the average current estimated for the generators on each muscle node for all the 11 contractions considered and are coloured based on their function. On the lower plot, the black dotted

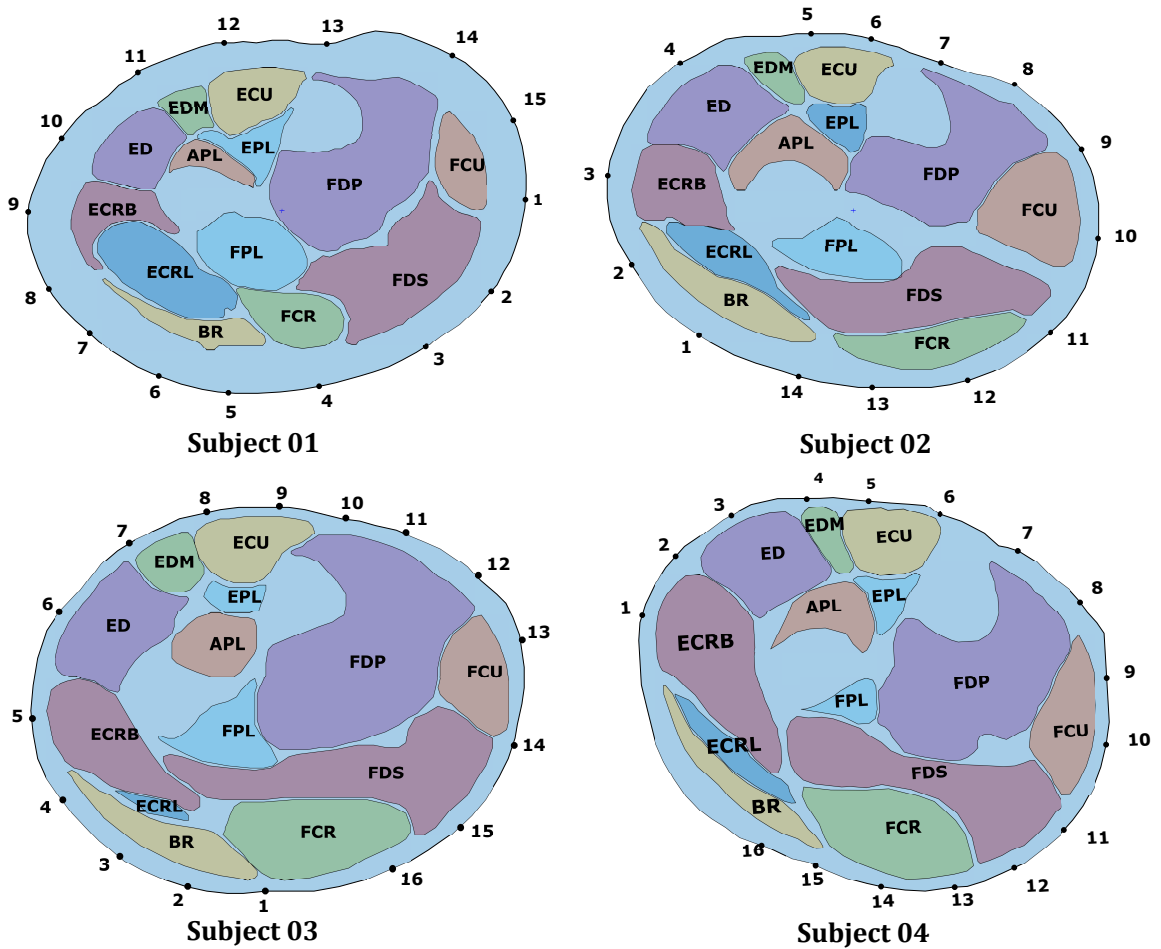


Figure 3-6: Results of the segmentation on muscles and registration of electrodes position on the 2D image plane of the MRI slice. In each MRI slice the following muscles can be identified : Abductor Pollicis Longus (APL), Extensor Pollicis Longus (EPL), Brachioradialis (BR), Extensor Digitorum (ED), Extensor Carpi Radialis Longus (ECRL), Extensor Carpi Radialis Brevis (ECRB), Extensor Carpi Ulnaris (ECU), Extensor Digiti Minimi (EDM), Flexor Digitorum Profundus (FDP), Flexor Digitorum Superficialis (FDS), Flexor Carpi Ulnaris (FCU), Flexor Carpi Radialis (FCR)

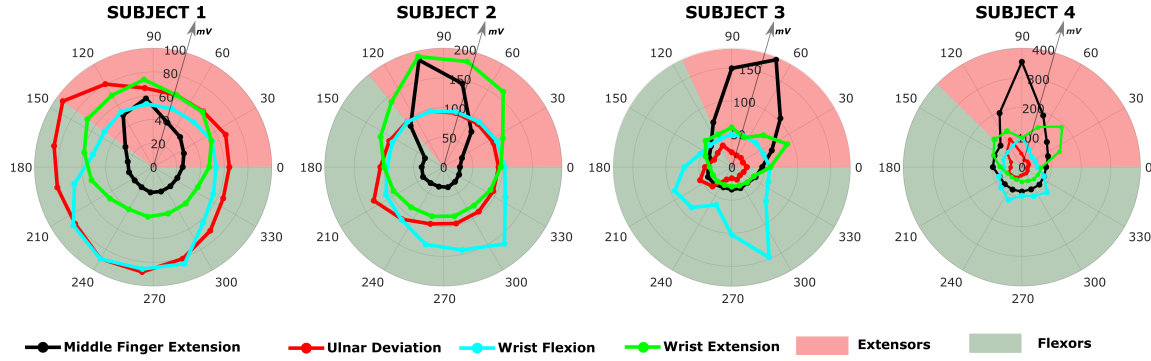


Figure 3-7: sEMG RMS profile for the four considered tasks at 50% MVC for all the subjects. Each isometric task profile is represented with a different color with a circle indicating the local value measured on the electrode. The electrodes are assumed to be equally distributed around the circumference of the cross section of the forearm. The posterior and anterior side, corresponding to the sectors where extensor and flexor muscles are located, are represented with different background color.

line represents the projection of the estimated currents on the voltage space whereas the measured sEMG is represented with a dashed red line. The background color is represented with red for electrodes on the anterior side, i.e. electrodes over flexor muscles, and green for electrodes on the posterior side, i.e. electrodes over extensor muscles. The number of electrodes is different for each subject and the number of electrodes of the anterior or posterior side changes depending on the subject.

A quantitative evaluation of the voltage fitting onto the electrodes space is reported with GOF values in Table 3.2 with the average value and the standard deviations over the 11 tasks considered.

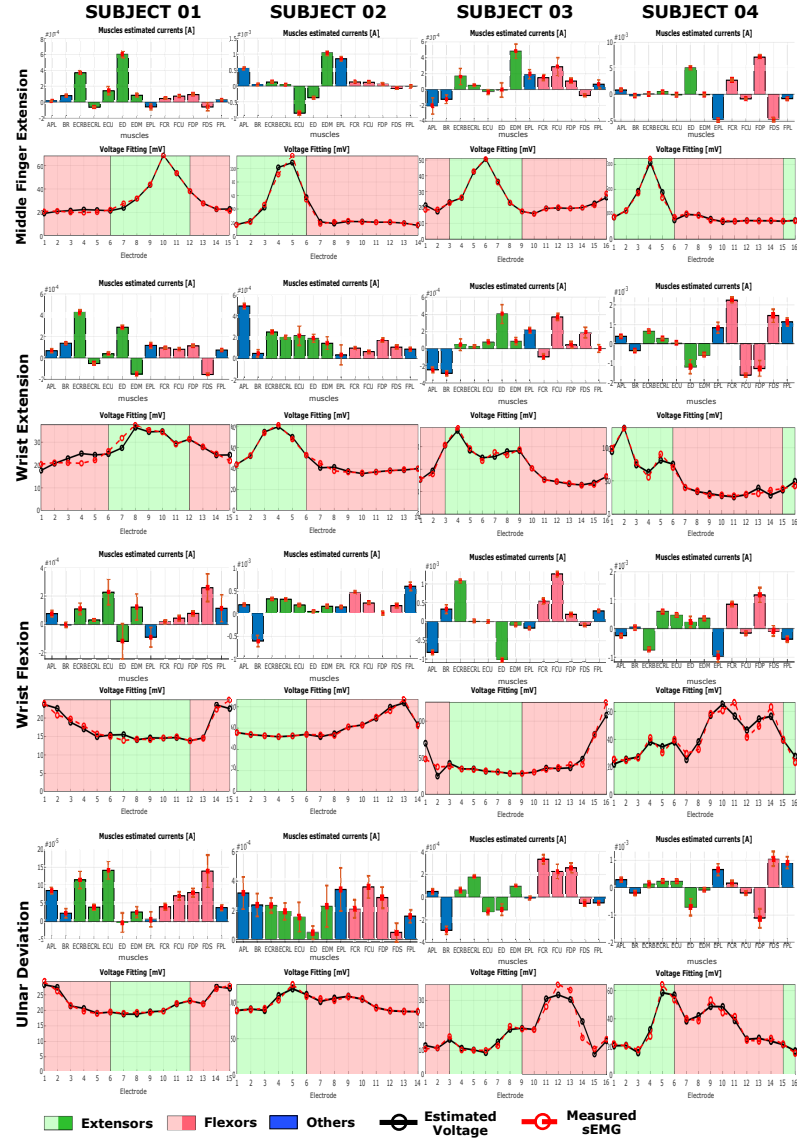


Figure 3-8: Estimated currents and voltage fitting on the electrodes space for all the tasks considered at 25% of MVC. Each bar represents the average current estimated for a muscle for 11 repetitions. The bar is coloured in green for extensors and in red for flexors. Muscles that are not mainly involved in the considered movements according to anatomy are colored in blue. On the electrodes space, the measured sEMG is represented with a red dotted line, whereas one example of the estimated value is represented with a solid black line. The background color is green for electrodes over the posterior side of the forearm (extensors) and is red for electrodes over the anterior side of the forearm (flexors). For further information on the meaning of the abbreviation of the muscles and their position refer to Figure 3-6.

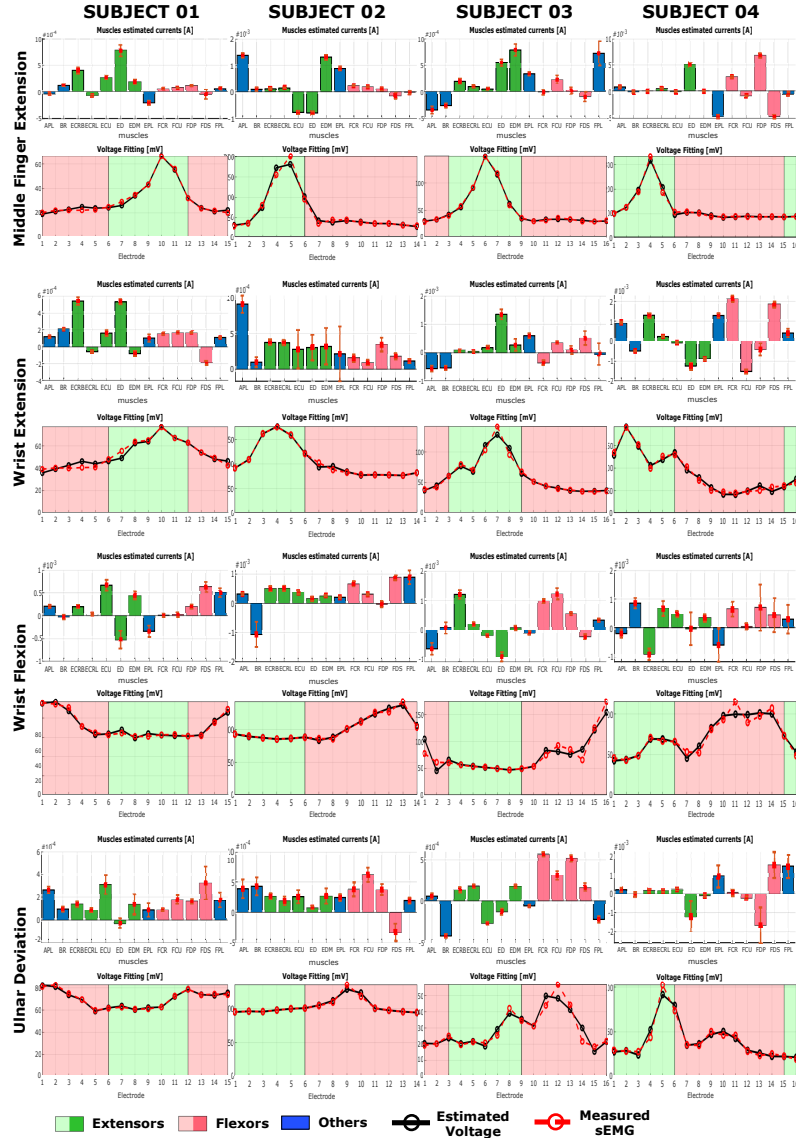


Figure 3-9: Estimated currents and voltage fitting on the electrodes space for all the tasks considered at 50% of MVC. Each bar represents the average current estimated for a muscle for 11 repetitions. The bar is coloured in green for extensors and in red for flexors. Muscles that are not mainly involved in the considered movements according to anatomy are colored in blue. On the electrodes space, the measured sEMG is represented with a red dotted line, whereas one example of the estimated value is represented with a solid black line. The background color is green for electrodes over the posterior side of the forearm (extensors) and is red for electrodes over the anterior side of the forearm (flexors). For further information on the meaning of the abbreviation of the muscles and their position refer to Figure 3-6.

Table 3.2: Goodness of Fit (GOF) value of the reconstructed sEMG value on the electrode space in terms of Normalized Root Mean Square Error (NRMSE).

	Subject 01	Subject 02	Subject 03	Subject 04
middle fing. ext (25% MVC)	$96.64 \pm 0.41\%$	$95.95 \pm 0.39\%$	$96.22 \pm 1.27 \%$	$97.90 \pm 0.17 \%$
middle fing. ext (50% MVC)	$97.06 \pm 0.55\%$	$95.81 \pm 0.34\%$	$98.18 \pm 0.26 \%$	$98.01 \pm 0.09 \%$
ulnar deviation (25% MVC)	$94.18 \pm 0.57\%$	$94.32 \pm 1.60\%$	$90.51 \pm 0.43 \%$	$95.45 \pm 0.53 \%$
ulnar deviation (50% MVC)	$96.27 \pm 1.34\%$	$95.45 \pm 0.84\%$	$89.63 \pm 0.67 \%$	$96.80 \pm 0.53 \%$
wrist ext (25% MVC)	$88.94 \pm 0.73\%$	$96.43 \pm 0.74\%$	$94.55 \pm 1.42 \%$	$96.27 \pm 0.23 \%$
wrist ext (50% MVC)	$92.48 \pm 0.67\%$	$96.37 \pm 0.60\%$	$95.11 \pm 1.73 \%$	$97.00 \pm 0.40 \%$
wrist flex (25% MVC)	$93.05 \pm 1.67\%$	$95.45 \pm 0.44\%$	$91.25 \pm 0.45 \%$	$90.91 \pm 0.90 \%$
wrist flex (50% MVC)	$92.91 \pm 1.08\%$	$94.78 \pm 0.50\%$	$89.25 \pm 0.96 \%$	$91.46 \pm 0.72 \%$

3.4 Discussion

Observing the plots in Figures 3-8 and 3-9 for each of the tasks, the inter-subject and inter-task differences can be seen [72–74]. For a given task, however, the group of muscles involved is not significantly changing between subjects, but it is possible to observe subjective characteristics in muscle activation. No significant changes can be observed in the activation pattern between different force level.

Each of the tasks shows specific muscle activation pattern that are in most of the case in agreement with what is reported in the anatomical literature. Each of the subject shows a subjective variation on the task activation pattern, especially for middle finger extension, (MFE), wrist extension(WE) and wrist flexion (WF) (Figure 3-8 and 3-9). Ulnar deviation (UD) shows a higher variability among subjects in both the estimated muscle pattern and in the input sEMG. UD could have a marked variability between subject depending upon the prono-supination and wrist flexion extension angle at which the subject have their neutral position. For a slightly flexed wrist, activation of the flexor muscles will be higher during ulnar deviation

when compared to slightly extended wrist.

During middle finger extension (MFE), for all subjects and in both force conditions a clear peak activity was registered on one or two extensor muscles, and for all subjects there was at least one muscle active among ED and EDM, indicated in the literature as major responsible for that task. In particular, looking at both Figure 3-8 and 3-9, for subject 1 there is a peak on ED with a lower peak on ECRB, on subject 2 there are peaks on EDM and EPL and a negative peak also on ECU, on subject 3 there is a clear peak on EDM, while on subject 4 the peaks are on ED and EPL, with this last one negative. During WE it is possible to observe a general activation of extensor muscles on all subject, with subject 1 showing a peak activation of ECRL and ED, subjects 2 showing a more homogenous activation among all extensors and subject 3 and 4 showing a sparse activation with clear peaks on, respectively ED for subject 3 and on ED and EDM for subject 4. On subject 2 a peak on APL can be observed as well. APL is not actively involved in the extension task but its activation can be due to the fact that the subject tried to spread the hand fingers, including the thumb, during the extension of the wrist. The fact that the activation pattern for subject 2, unlike the other subjects, is homogeneous among all extensors might indicate that the subject extended the fingers while trying to extend the wrist.

During WF, it is possible to observe a peak activation on FDS on subject 1, peaks on FCR, FCU, and FPL on subject 2, peaks on FCR and FCU for subject 3 while for subject 4 there is only a peak on FCR and FPD. These results are in accordance to the anatomical knowledge, and each of the subject uses a different muscle among the possible ones to perform the same task. Subject 2 shows an additional significant activation of BR, indicating that, probably, during the flexion of the wrist the subject

also tried to flex the forearm around the elbow joint.

For ulnar deviation (UD) results are according to anatomical knowledge in the case of subject 1, 2, and 3. In fact it is possible to observe peaks on either one or both of ECU and FCU. Subject 4 presents an activation on ED, EPL and FDP, while muscles that are indicated as main responsible for UD i.e. ECU, FCU, FCR, ECRL, ECRB, show a lower activation level. Observing the measured sEMG of UD for subject 4, it shows a different shape compared to the other subjects, indicating that the difference might be due to a subjective muscle activation pattern characteristic of that subject.

Observing both the estimated muscle activation profile (Figures 3-8 and 3-9) and the measured sEMG profile (Figure 3-7) around the forearm, each of the subjects perform each of the task in a characteristic way. Observing the input sEMG profiles it can be noted that for a chosen task there are important differences among subjects. The difference in the morphology of the forearm could explain different muscle patterns estimation. In the case of MFE, observing the sEMG profiles in Figure 3-7, it can be noticed that a similar profile shape among subjects is shared, where a single peak in the posterior side of the forearm muscles is present. For subject 2 the activation peak is shifted more toward the muscles on the anterior side, which might justify higher peaks on EDM and EPL. This means that all subjects performed the MFE in approximately the same way, activating either the same muscles or group of muscles around the same section of the forearm. On the other hand, a different relative activation is present, based on how the neural system of each subject adapted to perform that specific task. In the case of WE and WF, subject 1 and 2 show a measured voltage with a smoother profile around the arm, whereas subject 3 and

subject 4 present a more irregular profile with a biphasic behaviour. An even bigger difference can be observed for UD, where subject 1 and 2 present a rather smooth and flat sEMG with a peak on the flexor side of the arm, while subject 3 and 4 presents clear peaks. In particular subject 4 showed a biphasic sEMG profile with voltage peaks measured around electrodes 5 and 10 (Figure 3-8 and 3-9). Since UD, due to the nature of the movement, involves both extensor and flexor muscles, it can be seen that in general the peaks in the sEMG profiles are around the boundary area between extensor and flexors. However, each of the subjects present a characteristic shape, indicating that for this movement the muscle pattern might change significantly between subjects. The reason behind this apparent difference in the sEMG profile might be the position of the forearm with respect to the neutral position of each subject during the experiment. The supination angle of the forearm during the data collection might not have been perfectly horizontal causing a different activation of muscles.

Comparing the muscle signal patterns between 25% and 50% MVC conditions (Figure 3-8 and 3-9), they remain almost unchanged. This means that each subject maintain their specific muscle activation strategy among different force conditions. Each of the subjects therefore keeps activating the same muscles with the same strategy at different force levels, increasing the overall muscle activity of the involved muscles, without using other muscles or changing activation pattern. The method is therefore robust to different force conditions for the same task. However, it is important to notice that the force conditions and the choice of ignoring the first and the last repetition were meant to minimize the risk of having adaptation and fatigue effects. In fact, in case of adaptation and fatigue conditions the activated muscle

pattern might undergo changes due to a varying muscle recruitment pattern from the CNS[75–78].

The projection of the estimated current on the electrodes potential space fits the measured sEMG with a GOF over 90% for almost all of the task considered in both force conditions (Table 3.2). Thus, the currents estimated with the proposed model are able to explain on average more than 90% of the information enclosed in the RMS of the measured sEMG. Exceptions are WE for subject 1 at 25% MVC and WF and UD at 50%MVC for subject4, where GOF is slightly under 90%.

In different cases it is possible to observe a simultaneous activation of both agonistic and antagonistic muscles, i.e. flexors and extensors, thus co-contraction is happening. Furthermore, it is worth noting that in several cases, such as MFE, WE, UD for subject 4, MFE and WE for subject 1 or WE, WF, and UD for subject 3, currents with opposite signals are estimated for antagonistic muscles. Therefore, we hypothesised that the sign of the current is indicating the direction of the power exerted by the muscles. That would mean that the sign of the current is giving mechanical information of the system, such as the type of contraction of the muscles, which can be concentric or eccentric. The estimated voltages at the muscles nodes were all positive, therefore the sign of the electrical power of the network was defined by the sign of the currents. This is however, does not seem to be valid in general, probably because of the fact that for this work only an average behaviour has been considered. A study on the time series estimation of muscle pattern would help supporting this hypothesis and it will be further considered in the future.

Overall the results show that, for a chosen task, a small signal variance is estimated among tasks repetition. Thus, on average, each of the task has been performed

in the same manner by the subject. However, such as for UD at 50%MVC for subject 2 or WF at 50% MVC for subject 4, the estimated patterns show a higher variability, indicating that at each of the repetition significant differences in the contraction were happening.

The number of electrodes was different for all the subjects because of the different circumferences of each of the subject's forearms. The electrode sheets were therefore able to cover a different amount of the forearm circumference as it can be observed in Figure 3-6. Subject 1 and subject 3 show a uniform coverage of the forearm surface with 15 and 16 electrodes respectively. Subject 2 and subject 4 present regions that are not covered with electrodes. In particular, for subject 2 the density of electrodes is lower over the extensor side of the forearm, while for subject 4 there were fewer than two electrodes directly over BR, ECRL, and ECRB. For subject 2, the lower electrode density over the extensor side of the forearm might be responsible for the higher activation of APL observed during WE. The fact that only one electrode is collecting the information above ED and APL might have mislead the inverse algorithm in the estimation of the activation pattern. On subject 4, the width of the area not covered with electrodes is bigger than that of other subjects. In particular, between the electrodes 1 and 16, no electrodes is directly over ECRL. This does not seem to influence too much the estimation of the results for MFE, WF and UD, since, observing Figures 3-8 and 3-9, the sEMG values on electrodes 1 and 16 are low and of similar values. Since anatomically BR, ECRB and ECRL are not involved in these tasks, we can assume that the sEMG values in the electrode missing would be similar to that measured on electrodes 1 and 16. However, in the case of WE, ECRB and ECRL are muscles involved in the task. Observing the sEMG values on

electrodes 1 and 16, they show a different amplitude. Therefore, it may be presumed that between electrode 1 and 16 the sEMG value is not low. As a consequence, the lack of electrodes in that forearm portion might have caused a loss of information that influenced the muscle pattern estimation for WE.

Finally, it is important to notice that in this work, the role of the skin conductance was ignored. Skin is known to have a strong low-pass filtering effect on the sEMG signal. Since only the average behaviour was considered, we think that for the purpose of this paper, this did not have a big influence on the results. However, it is important to notice that it might have an influence on the general amplitude of the estimated currents, since the conductivity value of the skin is significantly lower than that of muscles and of fat tissue. For this reason, the value of the single muscle current cannot be considered a precise estimation of the muscle activity. However, the relative activation among muscles remain unvaried in the estimation process. With this work, we rather want to show new simple way to estimate the activation pattern of a set of muscles rather than focusing on the single muscles.

3.5 Proposed additional validation of the Resistance matrix

Based on what was presented in the previous sections, a key point of the discussion is about the validation. The type of information that needs to be validated and the characteristic of the anatomical part studied, i.e. high density of muscles and presence of both superficial and deep muscles, makes a direct validation impossible.

3.5. PROPOSED ADDITIONAL VALIDATION OF THE RESISTANCE MATRIX⁸¹

Therefore, in the previous section an indirect validation based on the comparison of the activation pattern with anatomical knowledge from literature and on the evaluation of fitting on the electrode space was proposed.

Even though the use of needle electrodes to record a ground truth might seem like a solution, this is not true in this case. In fact the information recorded with the use of needle electrodes would allow the recording of activities from a small portion of motor-units located closely the sensing tip of the needle. Therefore the information recorded would be extremely local and could not therefore be used as reference for the global activation status of the targeted muscle. It is therefore inevitable the use of indirect methods for the validation of the results.

In this section I propose an alternative method for the partial estimation of the system matrix describing the relationship between the muscles currents and the voltage measured at the electrodes that, in addition with the already proposed and used validation criteria, could give a stronger method to prove the previously exposed statements. The proposed validation method utilized the neuro-muscular electro stimulation (NMES) on muscles that could be stimulated from the surface i.e superficial muscle. Each of the accessible muscle is repeatedly stimulated with a known current pulse and the response that is recorded using a set of EMG electrodes wrapped around the circumference of the forearm. These values could be then exploited to estimate the values of the resistance in the constructed network.

For this section we utilized a commercially available electrostimulator, and this constrained the stimulation to only a limited muscles, practically allowing the activation of only the superficial set of the muscles represented in the MRI scan. As a consequence only part of the transfer matrix could be estimated. This however,

could still give a quantification and an indication, even if partial, of the resistances used to build the circuit and consequent validation of the proposed approach.

At the present time of this draft version, the method is only described from a method point of view, and the results are still under analysis and evaluation.

3.5.1 Methodology

The T1-weighted MRI of the participant's forearm was acquired with the subject in fetal position and the forearm of the target arm stretched above his head with a Siemens Prima 3T MR scanner (Siemens, Germany) at the Tokyo Institute of Technology (Ookayama, Ota, Tokyo) prior to the electro-stimulation experiment. The hand was kept with the palm facing upward in order to maintain the ulna and the radius parallel, consistently to the forearm position during the EMG acquisition. A field of view(FOV) of 192×192 mm was acquired and a slice thickness of 3 mm was set and saved on a 640×640 pixels matrix. A total of 96 slices were acquired for a total length of 288 mm covered along the longitudinal direction of the forearm. A set of 6 of vitamine E capsules were positioned on specific points forming a grid of reference points on the forearm, that was used for registration (Figure 3-10). Vitamine E is fat soluble and therefore has a high contrast in T1-weighted images. The repetition time was set to 10ms while the echo time was set to 3.69 ms.

3.5.2 Experimental Setup

One male healthy subject (24 yo) took part to the experiment. The participant was seated on a stool with the forearm laying on an external frame for support. The

3.5. PROPOSED ADDITIONAL VALIDATION OF THE RESISTANCE MATRIX⁸³

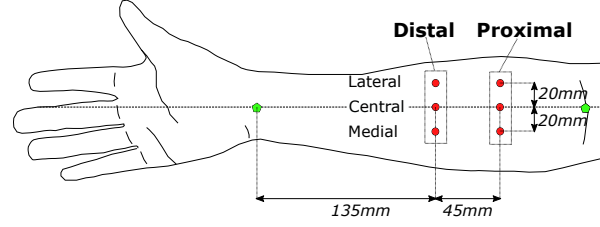


Figure 3-10: Position of the markers on the forearm

arm was kept in supinated position with the palm facing up in relaxed position. Previous to the experimental part, the position of the superficial innervation zones were identified through scanning procedure [60]. EMG was acquired with a couple of custom designed electrodes sheet wrapped around the arm. The sampling frequency of the EMG was set to 2000 Hz.

Since the EMS did not provide the specific value of the output current it had to be measured manually. To measure the current the terminals of the EMS where connected to the terminals of a known resistance and the EMS was activated with the same stimulation program used during the experiment. In order for the EMS to work, the resistance R was chosen so that it matched the resistance range indicated in the specification of the device. Two different resistances were tested to check the consistency of the measured current value. In particular resistances of 680Ω and 1000Ω were utilized. An oscilloscope was then used to measure the voltage at the terminal of the EMS. The voltage wave-shape was a biphasic rectangular wave with a peak voltage V_{MAX} . The peak current was measured using Ohm's Law

$$I_{MAX} = \frac{V_{MAX}}{R}. \quad (3.10)$$

For the subject that participated the experiment and the stimulation program

that was utilized, the measured currents were of 0.588mA for the 680Ω resistance and of 0.6 mA for the 1000Ω resistance. The average value of 0.594 mA was therefore assumed and utilized for the calculations.

Before applying the EMS it is important to locate the motor point of the muscles and to mark them so that they could be precisely stimulated. For the subject the motor point for the following 8 muscles was located :

- Palmaris longus (PL)
- Flexor Carpi Radialis (FCR)
- Pronator Teres (PT)
- Flexor Carpi Ulnaris (FCU)
- Flexor Digitorum Superficialis (FDS)
- Brachioradialis (BR)
- Extensor Digitorum (ED)
- Extensor Carpi Radialis (ECR)

The position was found with a scanning procedure using a pen with an catode on the tip. The position was chosen based on the strength and the type of the contraction elicited and on anatomical information from medical literature [71].

Once found the motor point of the muscles they were marked and the electrodes sheet were wrapped on the forearm in correspondence to the position marked during the MRI. Some of the motor point were however covered by the electrodes sheets and

were not accessible. These covered muscles were not reported in the muscle listed above.

After that the muscles were stimulated one by one with the the EMS. The stimulation pattern for each of the muscles foresaw an initial 10 seconds rest followed by 10 repeated stimulation lasting 3 seconds. Between consecutive stimulation a time of 5 seconds rest was given. For the stimulation of the extensor muscles, since these muscle groups are located on the posterior side of the forearm, it was held slightly bent in order to be able to access the motor points of the muscles.

3.5.3 Proposed validation of the system matrix

As reported in the previous chapter, the topology of circuit is described through the incidence matrix B . Weights are considered with a diagonal weight matrix that is used to calculate the Laplacian matrix \mathcal{L} as :

$$\mathcal{L} = B \cdot \text{diag}(w) \cdot B^T \quad (3.11)$$

where $\text{diag}(w)$ is the diagonal matrix of the weights of all edges, i.e. it contains the value of the conductance of all the resistances. The Laplacian matrix is a singular positive definite symmetric matrix where all the non-zero values are values of the conductances of the circuit. The currents and the voltage of the nodes are related through the relation seen in the previous chapter :

$$I = (\mathcal{L} + G)V = L_R V \quad (3.12)$$

where G is a diagonal matrix of shunt resistances, i.e. the resistances that are

connecting all the nodes to the ground. Since the voltage is measured only on the nodes corresponding to electrodes and the current we apply is only on muscles, it is possible to remove the rows corresponding to the electrodes and the columns corresponding to the muscles' nodes. The resulting matrix \tilde{L}_R will be of reduced dimension and it will only contain the values of the resistances that connects the superficial muscles stimulated with the electrodes. The resulting relation will be the following :

$$I_{\text{muscle}} = \tilde{L}_R V_{\text{electrode}} \quad (3.13)$$

where I_{muscle} is the vector of currents of the muscles, \tilde{L}_R is the reduced transfer matrix and $V_{\text{electrode}}$ is the vector of read EMG.

Since the current on the muscles is known and is equal to that outputted by the EMS, and the voltages are the values measured with the EMG. For each of the stimulation the peak voltages measured will be averaged and that will be considered to be elicited voltage.

Each of the current-voltage value obtained after a stimulation pattern define a system of linear equation where the unknown values are the coefficient of the \tilde{L}_R . Furthermore some of the values of the matrix are zero, corresponding to the non-existing edges between nodes. The resolution of the obtained linear system will provide an estimate of the value of the conductance for the available edges. A regression will be considered to identify the parameters of the system matrix.

3.5.4 Discussion

The proposed method aims to be able to provide a validation of the resistance values that composing the system matrix. It is a rather simple methodology to obtain an estimate of the resistances in the system. A matching between the resistance of the network with the resistances measured would be an additional proof of the validity of the method and along with the already provided validation method might be a robust enough way for validation. The majority of the muscles of the forearm is actually on the surface (9 out of 13) and therefore it could provide a way to estimate and calibrate the conductances value for a good part of the system matrix. In the future the use of invasive stimulation could be considered for the stimulation of the deeper layer of muscles.

3.6 Conclusions of this chapter

In this chapter I presented a novel method for the estimation of muscle activities. The activities were quantified using the muscle currents estimated in an electrical system created from subject specific MRI images. The model is able to provide an estimation of the relative activation for a set of muscles identified within an MRI section of the forearm, through the construction of a purely resistive electrical model of the conductive volume depicted in the slice. The results highlighted some interesting properties of the method in the estimation of subject muscle activation patterns for potential rehabilitation applications. For the same task the estimated pattern were similar among subjects, but subjective activation features can still be observed among

subjects, showing that the proposed method is able to capture anatomically valid muscle activation maintaining a subjectivity in the results that allows a comparison between different subjects. The input sEMG profiles changed with subject, reflecting the fact that each of the subject has a personal signature in the activation pattern, even if each of the single muscle maintain its properties and role. The proposed method is able to cope with this variability rearranging the muscle activation pattern to explain the input sEMG with a valid current pattern. Furthermore, the muscle patterns are not changing between different force levels, indicating that changes in the signal amplitude are not perturbing the estimated pattern. The estimated currents are able to explain over 90% of the input sEMG and the results have an anatomical meaning based on specialized literature and physiological consideration. The number of electrodes and their distribution might have had an influence in the estimation results. For two of the subjects the electrode density was lower in particular sections and this might have lead to different interpretation of the sEMG in the solution of the inverse problem.

Additionally, a complementary validation method was proposed with the use of electrostimulation in order to assess some of the components of the system matrix, exploiting the linearity of the system and a majority of muscles on the surface.

With this work we wanted to introduce a novel idea for solving the problem of estimating deep muscle activities. We used a simple electrical model, providing results obtained using a dataset acquired from healthy subjects. The proposed model inherently includes information about each of the subject inner morphology described in a simple and intuitive way. Furthermore, the rules defined for the model construction and for the estimation can be easily automatized making the translation of the

presented logic into a software routine with a low number of parameters.

The results shows that, for most of the task considered, the estimated muscle patterns are anatomically plausible. For simple static tasks, such as MFE, the estimated pattern, even if with a clear difference among subjects, provides an activation pattern that matches what is reported in the literature. In case of WE and WF, most of the case considered are anatomically consistent. However, some isolated results are uncertain. For UD, subject 1 and 2 shows valid results, while subject 4 shows different results, most likely due to a different sEMG profile around the arm, which indicate a different overall muscle activation, or an insufficient number of electrodes.

Several aspects of the model can still be improved, starting from the modeling to the estimation algorithm. In this work, we rather wanted to focus on the presentation of a different approach to exploits both information from MRI and sEMG to build a model able to solve the problem of muscle activity estimation, with a validation on a pool of healthy subject and with different movements in order to assess the performance that can be achieved with a simple and intuitive modeling. The impossibility to have a ground truth remain a challenging part for the validation of the method and it will be addressed in the future with the use of the method proposed at the end of this chapter.

Another important aspect that needs to be clarified regards the robustness of the method to electrodes malfunctions or to noisy channels. In the use of EMG these problems are quite common and therefore need to be considered. Furthermore it is important to evaluate how the number and the position of the electrodes with respect to specific muscle groups is influencing the performance and the estimation of the method. This is important for a more applicative reason, since for application

such as prosthetic, the number of electrodes from which the primitive information is collected is crucial. These issues will be discussed more thoroughly in the next chapter.

Finally, for this chapter the RMS of the sEMG during contraction was considered in order to give an average estimation of the behavior of the muscles during the selected tasks. In chapter 5 the time dimension will be introduced in the study to allow observing the contraction strategies of the muscles during the task execution.

Chapter 4

Effect of Electrodes Distribution

4.1 Introduction

In the previous chapter the electrical model and the current estimation method were thoroughly described. The model is created translating the information from a single MRI slice of the person into a network of resistances describing the signal transmission between neighbor elements in the volume conductor. The resulting system is linear and can be solved using a minimum norm approach. In order to consider the different contribution that big muscles can give compared to small muscles in the production of the surface voltage, a regularization based on the cross-sectional area of muscles observable on the MRI slice was utilized. The method's performance were evaluated on the experimental data of four healthy participants performing four isometric movements at wrist joint and MCP joint level.

However it still remains unclear how the position and the number of electrodes around the forearm are influencing the methods performance, i.e. how robust is the

method to electrodes shift or malfunctions. Signal disturbances and electrodes fault are not uncommon and can be caused by different elements such as the presence of artifacts of various types or to some defect in the electrode-skin contact. For this reason it is important to assess the effect of the number and of the position of the electrodes on the performance of the method. It is important to understand whether a high number of electrodes is necessary or whether their number can be diminished or optimized without heavily impacting the estimation capacity of the method and whether the performance of the methods might depend on the placement of the electrodes over specific group of muscles.

In this chapter I describe an analysis on the effect of changing the number of electrodes considered. In particular the aim is to verify the robustness of the method to different electrodes' configuration and to assess which position around the forearm are fundamental for the quality of the estimation or, conversely, whether electrodes in specific position could be instead removed without significantly influencing the performances.

From an application point of view, the number of electrodes is also of particular importance. In fact, the number of electrodes that needs to be applied strongly contribute to the portability of devices that utilize EMG, such as prosthetic. The number of electrodes actually utilized on commercial prosthetic devices is usually small [79], because the current state of the art prosthetic utilizes bipolar surface electrodes on top of specific muscles. At the moment, there is no record of commercialized prosthetic making use of high-density sEMG to collect muscle signal. It is therefore important to limit the number of electrodes utilized to make the use of HD-sEMG more attractive for prosthetic applications. The method proposed use a

limited amount of HD-sEMG electrodes, in particular, it makes use of single rows of electrodes without the need of a specific positioning. This makes its applying easier and in perspective ideal for commercialization since the electrodes row can embed in an elastic structures, similarly to other products in the market as the MyoTM (North Inc., Kitchener, Ontario, Canada).

The method's ability to estimate the whole spectrum of muscles in the MRI would potentially allow a better use of prosthetic since the role of all muscles, including deep muscles, could be taken into account. Therefore, in order to reduce the gap between the method and its applicability in real contexts, there is the need to assess the role of the number and the position of electrodes that are needed for the method to have a reliable estimation power.

The analysis is carried out considering the results of the estimation method while removing specific patterns of electrodes from the electrodes sheets and recalculating the resulting network. The number of electrodes that was removed, was chosen in order to avoid the under-determined case in the inverse problem thus keeping the number of electrode greater than or equal to the number of muscles. In order to have a complete view of the effect of the electrodes' removal, the analysis is done in both the electrodes space and on the muscles' space. The error in the electrodes' space is evaluated re-projecting the muscle currents calculated with the reduced network through the complete network to have an estimation of the complete set of electrodes. On the other side, the error on the muscle space was quantified observing the difference in the muscle activation patterns between the reduced and the complete network. The obtained EMG reconstruction is then compared with that obtained with the complete network in relation to the measured EMG. Furthermore, the effect

of removing equally spaced electrodes along with all the possible shift is evaluated to consider the effect of a different local electrode density. The dataset presented in Chapter 3 was used for this analysis. Since the number of electrodes change for each of the participants due to a different forearm circumference, the analysis was carried out on each subject separately, considering the effect on each different task with no regards on the force level.

Results showed that the regions were the extensors muscle group and the flexor muscle group interface is important in terms of information reconstructed, and removing electrodes in those areas leads to a consistent decrease in the performance. Tasks involving extension, i.e. middle finger extension and wrist extension, showed that electrodes removed from the extensor side lead to an increase in the method's performance. Conversely the removing of electrodes from the flexor side lead to a decrease in performance. This phenomena is attributable to a strong signal on the extensor side during extension so that the actual density of electrodes can be decreased. The wrist flexion did not show an analogous effect, most likely due to the fact that flexion task can be performed with different parts of the flexors, ulnar or radial or both.

The overall behavior with a decreasing number of electrodes showed an expected decrease of the performance for all subject, except for one who showed a different behavior with a decrease of the error when 1 electrode was removed. However, since from that subject only one electrode could be removed, the behavior for additional electrodes could not be determined.

On the muscle space the estimations showed generally a certain level of robustness against the removal of single electrodes. However different cases were highlighted

were the quality of the estimation was disrupted with particular configuration, indicating a certain level of subjectivity. The observation of the median calculated on different muscle groups showed that the removal of the electrodes on the activated side is not always having a bigger influence on the target muscle, but, on the contrary, different cases are emerging where the opposite is happening. The reason why this happen is not completely clear but different causes could be considered. The different size of the muscles for each subject under the same electrode density could be one of the reason as well as a local lower electrode density. Furthermore the presence of hidden preferential paths could be another reason for this behavior.

What emerges is that in general a reduction of the electrode density on the extensor and an increase on the flexors could be a good trade-off solution to increase the robustness in term of muscle estimation without reducing excessively the reconstruction power over the electrodes space. It will be also important to cover the surface where extensors and flexors are interfacing in order to be able to correctly discriminate the flexor and the extensors contribution.

The analysis and the results of this study will be used for later publication and therefore are not disclosed in this abridged version of the thesis.

THIS PAGE INTENTIONALLY LEFT BLANK

Chapter 5

Dynamic movements case

5.1 Introduction

In order for the proposed approach to be considered for a potential application it is crucial to consider not only the average behavior but its performance with the time dimension. In chapter 3 the method for isometric movements was developed and explained with the estimation of average performance. In chapter 4 the effect of the position and the number of electrodes on the methods performance were evaluated.

In this chapter we move a step forward towards the demonstration of the applicability of the method. In particular we introduce the time dimension to study the behavior of the method over time and how the method estimates each of the muscle's time series. The results of a first application of a windowing approach on a new EMG dataset acquired for 3 dynamic motions of the wrist. The results show that the method is able to obtain meaningful muscle pattern estimation for wrist flexion/extension, and partially valid patterns for ulnar deviation. The method is able

to explain over 95% of the input information from the EMG. The elaboration time was largely below the threshold of the electro-mechanical delay making it suitable for application of real time device control.

This work will be further extended in the full version of the thesis with the collection of data from more subject with dynamic movements.

5.2 Methodology

In this section experimental setup, data acquisition and model definition are described for a single male healthy subject. In particular, the MRI acquisition is described in the *MRI acquisition* section, the setup used to collect the sEMG and the motion capture data are described in the *Experimental Setup* section, the design of the electrical model is described in the *Electrical Model* section, the estimation of the muscle currents pattern is described in the *Muscles' current pattern estimation* section while the validation criteria are described in the *Validation* section.

5.2.1 MRI acquisition

A single healthy male person (24 yo, 47.6 kg, 1.60 m) participated the experiment. The experiment was approved by the ethical committee of the University of Tokyo. A T1-weighted MRI of the participant's forearm was acquired with a Siemens Prima 3T MR scanner (Siemens, Germany) at the Tokyo Institute of Technology (Ookayama, Ota, Tokyo) prior to the experiment. The information about the MRI scan and the imaging parameter set are those presented in chapter3. Please refer to section 3.5.1 for more details.

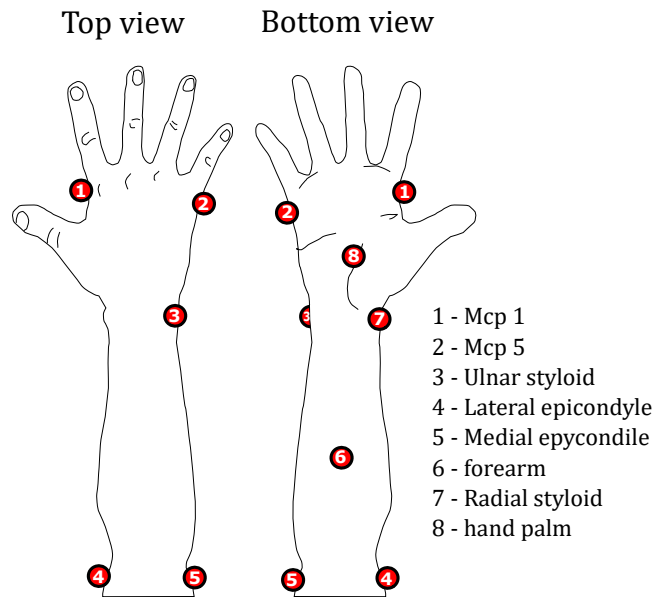


Figure 5-1: motion caption markers

5.2.2 Experimental Setup

For the recording of the EMG and the kinematics, the participant was seated on a stool with his forearm laying horizontally on a custom made frame with the relaxed outside the boundary of the frame so that the wrist movements were unfettered. A set of 8 markers were attached to the forearm and hand of the participant (Figure 5-1).

The markers' movements were tracked with a set of 10 Kendrel motion capture cameras (Motion Analysis, USA) arranged around the experimental area. The subject had to perform 10 repetitions of 3 different wrist movements:

1. Wrist extension

2. Wrist flexion
3. Ulnar deviation

The participant was asked to perform one repetition every 5 seconds and to hold the position for 3 seconds. Between two different task the subject rested for 120 seconds. Every movement was performed at self-selected speed.

5.2.3 EMG data

Muscle signals were acquired using custom made electrode sheet designed for this experiment. Each sheet contain a single row of 32, 5×5 mm, square electrodes with 5mm inter-electrode distance. The position of MRI markers, forming 2 rows, were identified on the forearm. For each marker row, 2 electrode sheet were wrapped around the forearm side by side so that the medial line of them was aligned with the line identified by markers position. The distance between the 2 electrodes sheet was set to be 10 mm. Since the lenght of the electrode sheet exceded the circumference of the forearm, some electrodes were overlapped. Overlapped electrodes were discarded in the signal processing step. For the purpose of this work only the distal electrode sheet of the distal marker sheet pair was considered.

The EMG signal was collected with an RHD2000 interface board (Intan Technologies, USA) at a sampling frequency of 2000 Hz. The acquired signals were processed offline on Matlab (Mathworks, USA) with a 4th order Butterworth filter between 4 to 450 Hz to cancel motion artifacts and high frequency noise.

5.2.4 Segmentation and Registration

An MRI slice was selected for segmentation in correspondance of the selected electrode sheet selected on the distal markers row. The segmentation is a process through which the boundaries of the muscles in the MRI slice are identified. Segmentation was done with ImageJ [66] based on information from specialized literature.

The following muscles were identified : Abductor Pollicis Longus (APL), Extensor Digitorum (ED), Extensor Digiti Minimi (EDM), Extensor Carpi Ulnaris (ECU), Extensor Pollicis + Extensor Indicis (EP+EI), Flexor Digitorum Profundis (FDP), Flexor Carpi Ulnaris (FCU), Flexor Digitorum Superficialis (FDS), Flexor Carpi Radialis (FCR), Pronator Teres (PT), Flexor Pollicis Longus (FPL), Brachioradialis (BR), Extensor Carpi Radialis Brevis and Extensor Carpi Radialis Longus (ECRB + ECRL).

The position of the electrodes on the MRI scan was defined with a registration process. The inter-electrodes distance and the position of the first electrode are known, since each electrode sheet was wrapped with the first electrode in correspondance to the medial marker. The boundary of the forearm and the position of the markers were set during the segmentation. The positions of the electrodes on the MRI slice were then calculated so that the first electrode was in correspondance to the projection of the medial marker on the surface of the forearm and the successive were positioned at increments of one inter-electrode distance from each other around the section of the forearm.

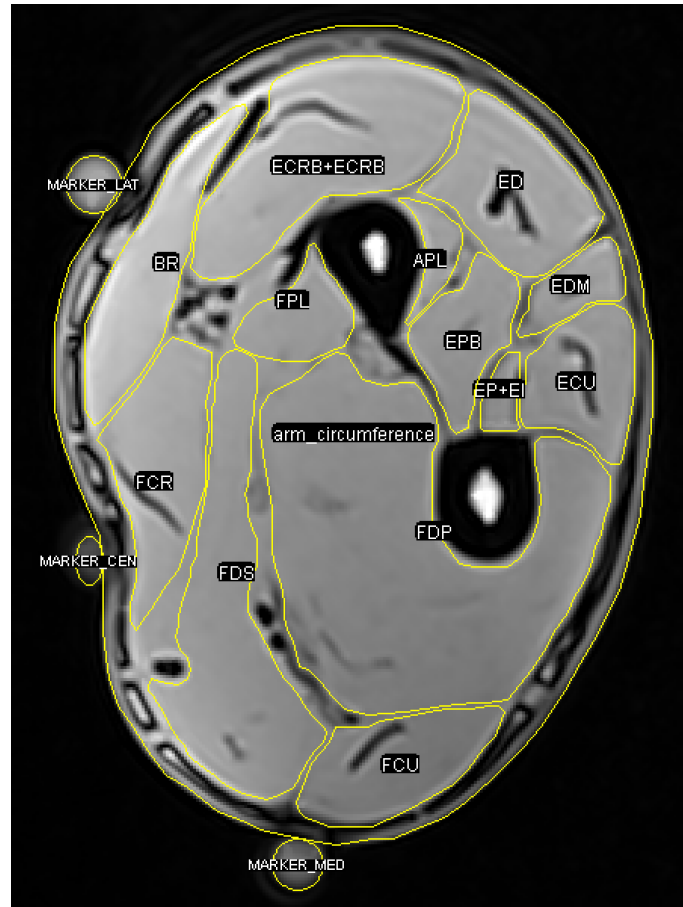


Figure 5-2: Segmentation results. 14 muscles can be identified : Abductor Pollicis Longus (APL), Extensor Digitorum (ED), Extensor Digiti Minimi (EDM), Extensor Carpi Ulnaris (ECU), Extensor Pollicis + Extensor Indicis (EP+EI), Flexor Digitorum Profundus (FDP), Flexor Carpi Ulnaris (FCU), Flexor Digitorum Superficialis (FDS), Flexor Carpi Radialis (FCR), Pronator Teres (PT), Flexor Pollicis Longus (FPL), Brachioradialis (BR), Extensor Carpi Radialis Brevis and Extensor Carpi Radialis Longus (ECRB + ECRL). Furthermore the position of the 3 markers is visible on the skin surface

5.2.5 Electrical Model

The method proposed describes the conductive volume using an electrical network. For the frequencies in which the sEMG signal works, the quasi-static approximation is valid and therefore capacitive and inductive effects in the tissues can be neglected, thus allowing to assume the volume conductor as purely resistive [28]. The model presented in chapter 3 can be therefore considered for the study on dynamic phenomena involving the time dimension. Since no reactive effects are considered, the skin kept been included into the fat thickness.

The electrical model presented describe the relation between the currents at the nodes \mathbf{I} and the voltage at the nodes \mathbf{V} which can be described according to the following relation:

$$\mathbf{I} = (\mathcal{L}_R + \mathbf{G})\mathbf{V} \quad (5.1)$$

where \mathcal{L}_R is the conductance matrix and \mathbf{G} is a matrix containing the shunt conductances of all nodes. Assuming that \mathbf{G} has at least one non-negative element, Equation 5.1 can be inverted :

$$\mathbf{V} = (\mathcal{L}_R + \mathbf{G})^{-1}\mathbf{I} = \mathbf{F}\mathbf{I} \quad (5.2)$$

with $\mathbf{F} = (\mathcal{L}_R + \mathbf{G})^{-1}$ is the system matrix.

5.2.6 Muscles' current pattern estimation

The muscle currents are estimated as the currents at the muscles' nodes. From Equation 5.2 it is possible to simplify the system to consider only the electrode voltage $\mathbf{V}_e \in \mathbb{R}^{n_e \times 1}$ and the muscles' nodes current $\mathbf{I}_m \in \mathbb{R}^{n_m \times 1}$:

$$\mathbf{V}_e = \tilde{\mathbf{F}} \mathbf{I}_m \quad (5.3)$$

where $\tilde{\mathbf{F}}$ is obtained from \mathbf{F} deleting the row corresponding to non electrodes nodes and the columns corresponding to non muscle nodes. To have a continuous estimation over time, a moving window was used. The window width was set to 128 samples with an overlap of 75%. In each of the windows k , the root mean square of the voltage vector $\mathbf{V}_e^{RMS}(k)$ was calculated, to be then used to solve the inverse problem. The inverse problem is overdetermined because the number of electrodes is bigger than the number of muscles. Therefore a regularization must be imposed in order to find a unique stable solution. The assumption of having a higher activation of bigger muscle was considered, and therefore muscles with smaller cross sectional area on the MRI were penalized. The muscles currents were therefore estimated as at each window i as:

$$\hat{\mathbf{I}}_m(i) = \tilde{\mathbf{F}}^T (\tilde{\mathbf{F}} \tilde{\mathbf{F}}^T + \lambda \mathbf{I})^{-1} \mathbf{V}_e^{RMS}(i) \quad (5.4)$$

where λ is the regularization vector that models the penalization, and is set to be a vector containing the inverse of the cross sectional area of all muscles.

5.2.7 Validation

A direct validation of the results would involve invasive insertions of electrodes in each of the muscles. Even if previous studies [9] utilized this approach, the high number of muscles involved in this study make it practically impossible. The method was therefore validated as described in chapter 3:

- I comparing the muscle activation pattern with anatomical information from literature
- II assessing the fitting of the reprojection of the estimation on the electrode space with the measured EMG data.

The anatomical information comparison was carried out comparing the estimated muscle currents with the muscle described as responsible for the movements in specialized literature [70, 71] :

- Wrist flexion : **FCU**, **FCR**, APL, EDM
- Wrist extension: **ECU**, ECRL, ECRB, ED
- Ulnar deviation: **FCU**, **ECU**, FCR, ECR

where the muscles mostly responsible for the movement are highlighted with bold font. Secondly, the method performance over time were evaluated with goodness of fit (GOF) between the muscles currents re-projected over the electrode's space and the output of the window application on the sEMG:

$$GOF = \frac{1}{W} \sum_w (1 - NRMSE(k)) = \frac{RMSE(k)}{max_k - min_k} \quad (5.5)$$

where $NRMSE(k)$ is the normalized root mean square error calculated on the window k and max_k and min_k are, respectively, the maximum and minimum value observed in the window k .

The estimated muscles currents profiles are represented in figure 5-3 for wrist flexion, figure 5-4 for wrist extension and figure 5-5 for ulnar deviation.

Observing Figure 5-3 the peak activity is registered on FCU, ECU and FDP. A lower activity can be observed on EP+EI. The activation on FCU is in accordance to anatomical information. The activation of ECU is compatible to a co-contraction phenomena. The low activation of FCR can be due to the fact that the participant flexed the wrist more towards the ulnar side, therefore focusing the activation of only the ulnar side of flexors. The absence of co-contraction on ECRL+ECRB further support this hypothesis. The peak on FDP indicates that the participant flexed the fingers as well while trying to flex the wrist.

Wrist extension activation (Figure 5-4) show a peak activation on ECU, ED, FPL and EPB. This is in accordance with the anatomical information where ECU is indicated as the main responsible for the wrist extension. ED is another muscle partially responsible for wrist extension. The simultaneous activation of FPL and EPL indicate that the participant tried to extend the thumb while performing the task

The currents estimation for ulnar deviation showed generally noisier results, with high activities registered on FCU, ECU, FDP, ED and EDP. The use of ECU and

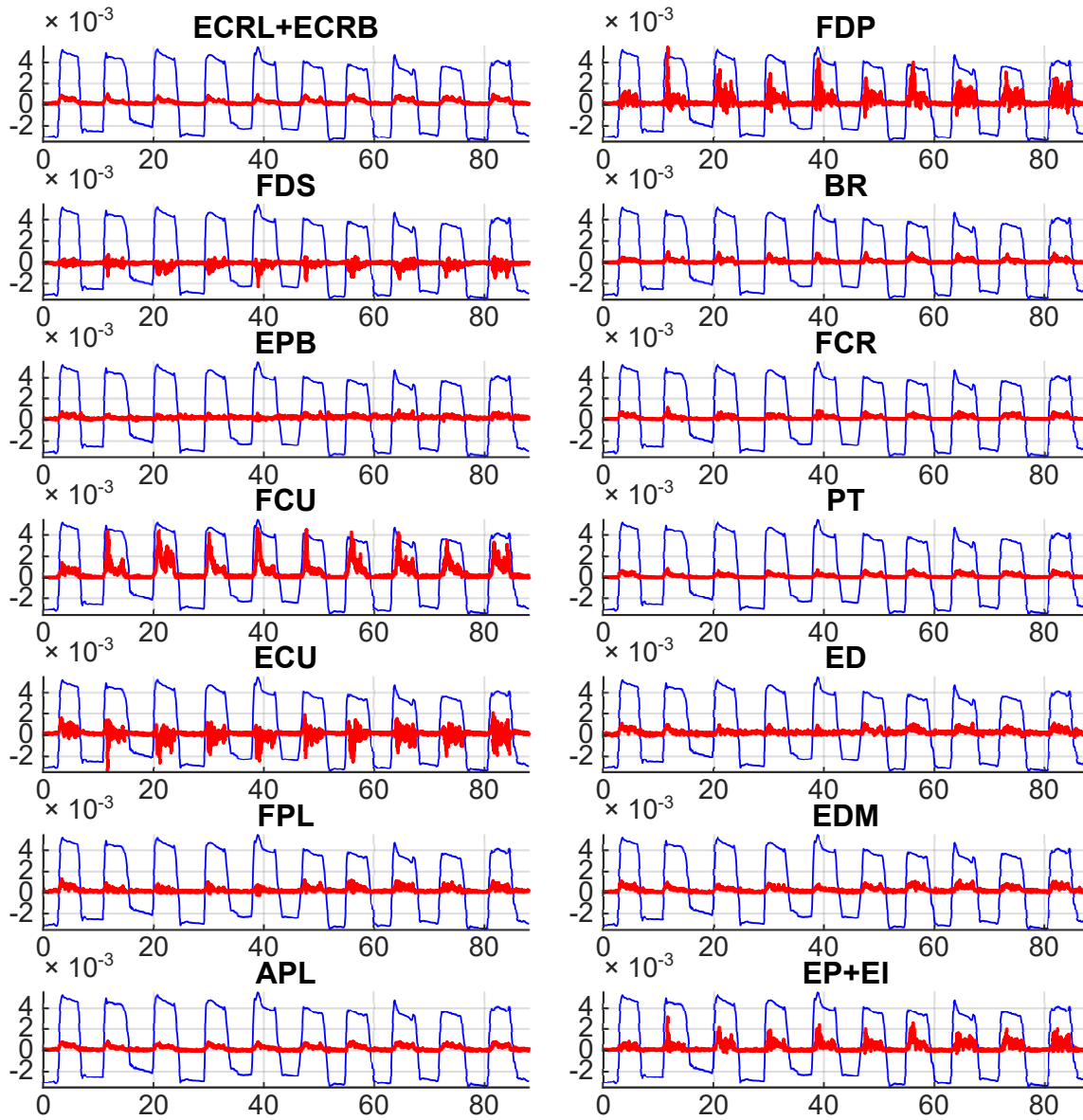


Figure 5-3: Estimated currents of all muscles for 10 repetition of wrist flexion task.

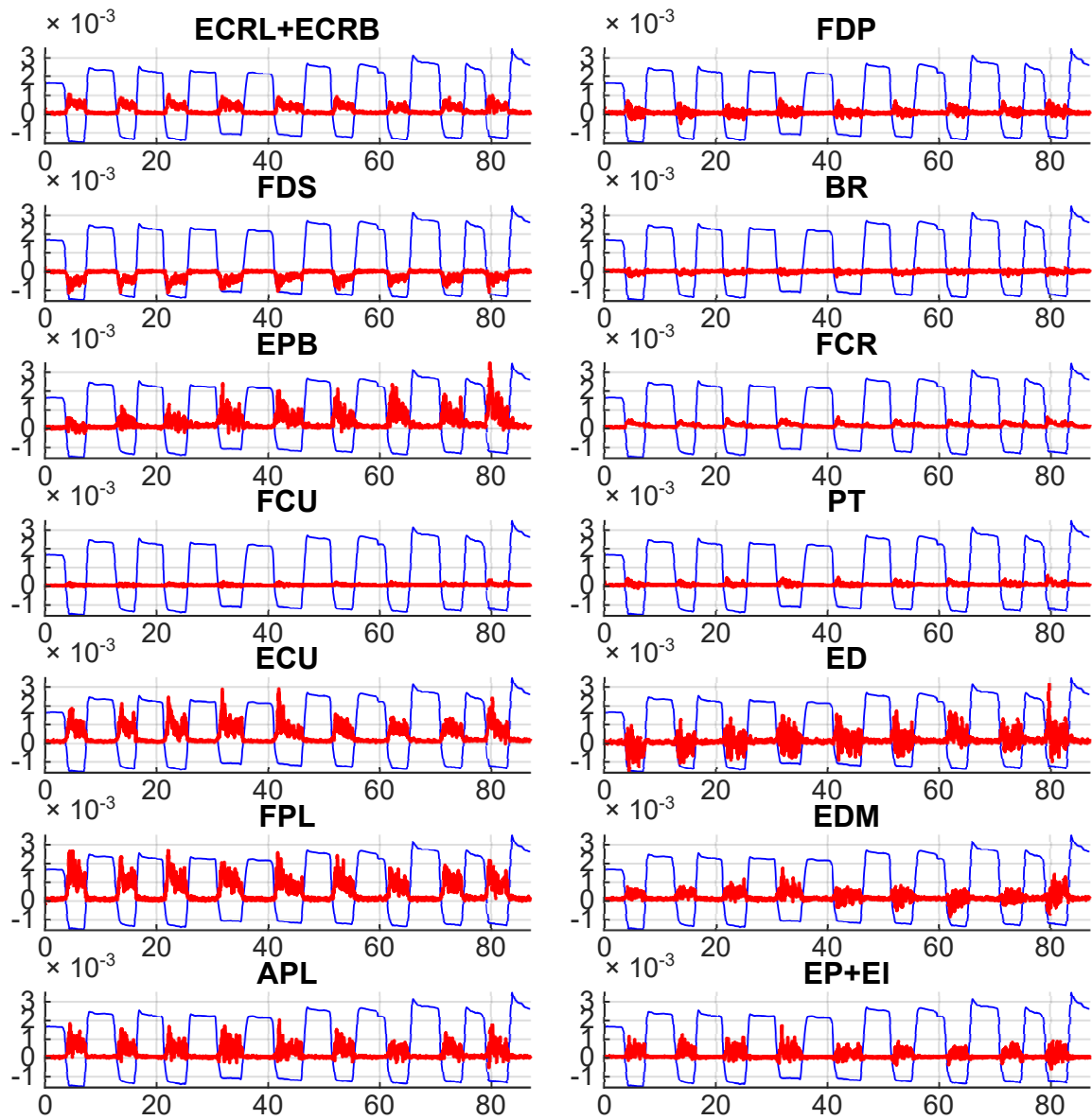


Figure 5-4: Estimated currents of all muscles for 10 repetition of wrist extension task.

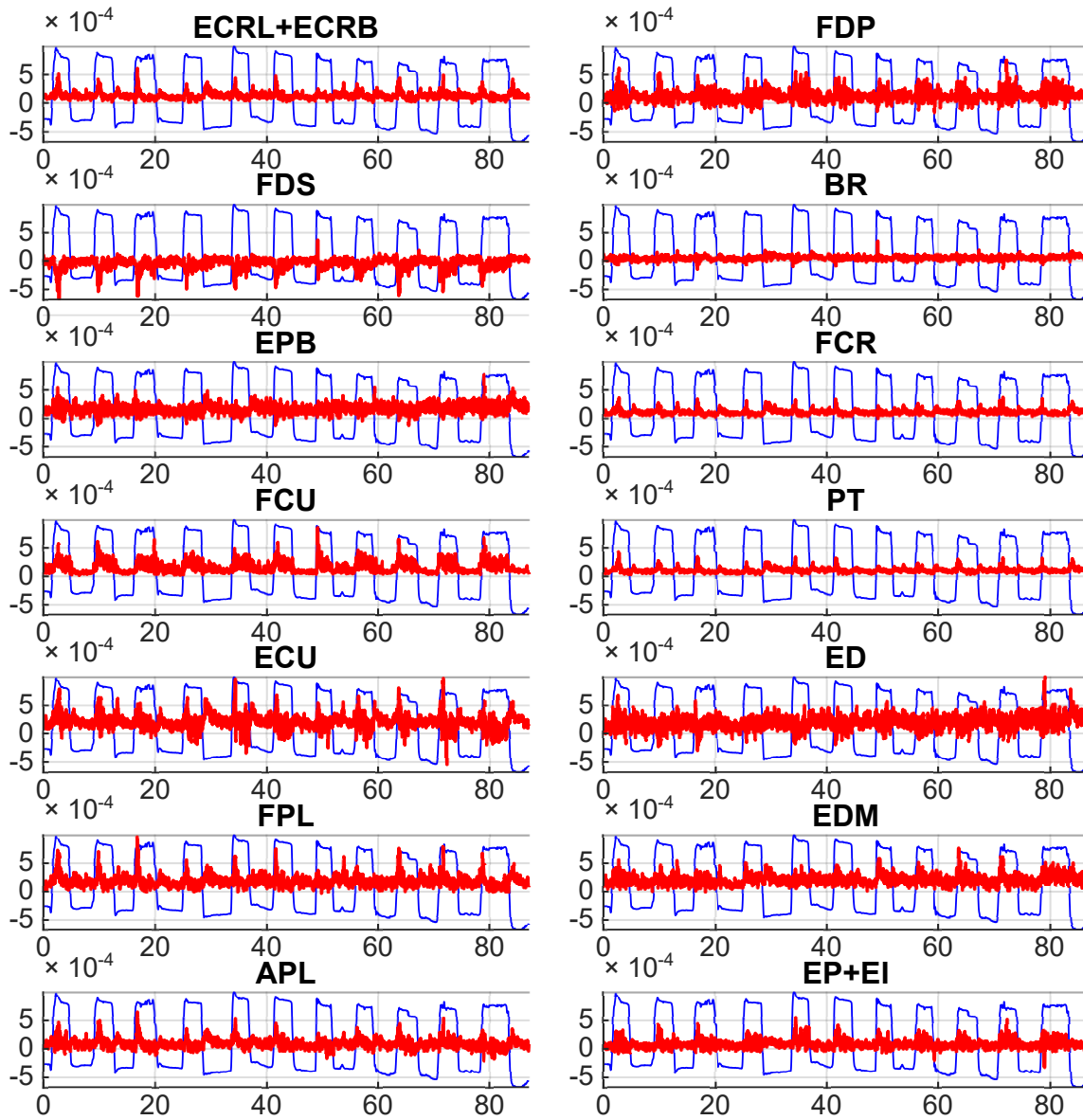


Figure 5-5: Estimated currents of all muscles for 10 repetition of ulnar deviation task.

FCU is compatible with what is reported in literature. The activation of finger muscles can indicate that the subject tried to hold the fingers straight while performing the task. Thumb muscles, such as EPB and FPL, also present a significant activity, probably due to some thumb movements during the ulnar flexion, likely a thumb extension.

The average GOF recorded over all electrodes were of $97.3 \pm 1.5\%$ for wrist extension, $95.3 \pm 2.4\%$ for wrist flexion and $96.6 \pm 1.5\%$ for ulnar deviation. The average elapsing time for one time window was of 0.82 ms. All the processing was done on a laptop equipped with an Intel Core i7 8650U processor.

5.3 Discussion

The estimated currents magnitude have a correspondence in anatomical information for wrist extension and wrist flexion. For ulnar deviation the results have a partial anatomical correspondence, however some uncertainties remain. These results agree with what has been previously observed for isometric contraction in [1] where the estimation for ulnar deviation showed a high variability. The results indicate that the participant performed the task using a subjective pattern of muscles, which can be due to a subjective neural control strategy as well as to the fact that the subject was not given any constraint on the movement, but was asked to perform the tasks naturally.

The sign of the estimated currents is either positive or negative. In some cases the currents are oscillating between positive and negative. A possible explanation for this rely on the duality that exist between a mechanical system and an electrical

network. In particular, since the RMS voltage of the electrodes are positive, the sign of the currents identify the sign of the power at that node. As a consequence, negative currents indicate power absorption while positive currents indicate power dissipation. Since there exist a duality between mechanical systems and electrical system, the electrical power of the network can be thought as mechanical power of the musculoskeletal system. In particular, since the muscle force is acting only in one direction, the sign of the power would indicate the sign of the velocity, therefore giving information on the type of contraction, whether concentric or eccentric. A way to verify this hypothesis would be to use ultrasound imaging while performing the task. This would provide information of the contraction type from the muscle fiber movement direction.

The estimated current for a single muscle cannot be considered as its activation. This is because the effect of the skin was ignored and therefore the amplitude of a single current will represent the activation of the muscle save for a constant. The relative currents amplitude, however, remains untouched, therefore the muscle activation patterns information is valid.

While the estimated currents are obtained through a regression and therefore, could be considered a validated measure that account for an extremely high variance accounted for, it could be further improved. The difficulties in having access to all forearm muscles information however, hinder the use of EMG for validation. A possible solution would be the use of musculoskeletal modeling to simulate the motion and use a static optimization to estimate the muscle activations. Another more direct and reliable approach would be the use of ultrasound imaging, since there is a relationship between the thickness of the muscle and its activation [80].

5.4 Conclusions of this chapter

In this chapter we presented the extension of the method introduced in 3 [1] for the estimation of muscle activation patterns over time for dynamic wrist movements. The method was applied on a dataset of one single healthy male subject. The results show that the method is able to provide muscle activation over time that can explain over 95% of the input EMG. The activation patterns have a correspondence with known anatomical information for wrist extension and flexion. The ulnar deviation present some uncertainties on the interpretation of the results. Muscle currents are estimated with either positive or negative currents and the interpretation of the current sign is still to be clarified, but we hypothesized that, in light of the electro-mechanical system duality, it could be related to the type of contraction that the muscle is undergoing to.

The use of ultrasound imaging would provide a way to better clarify these uncertainties. It would in fact allow the visualization of muscles during the contraction task, allowing a direct monitoring of the fiber motion for a more direct information for validation purposes.

Chapter 6

Conclusions and Future Works

6.1 Conclusions

In this thesis I proposed a novel method to construct a simple linear model that can be used to translate the morphological information of an MRI slice into a simple resistive network. The interaction between the structures and tissues inside the forearm are modeled analogously to a power grid, exploiting then the properties of the circuit and graph theory to estimate the muscle activation pattern. With this method the imaging power of the MRI is exploited to actively contribute for the creation of a model to estimate the activation of all muscles, including deep ones, which are ignored in the state of the art methods using EMG. The role of deep muscles is of strong importance for in different body parts, such as the lower back and the forearm, and the presented method provide a way to exploit EMG information to study them.

The proposed method propose a merging between MRI and EMG information

different from other approaches that previously aimed to create a hybrid method. It overcomes the limitations of the low time resolution of the mfMRI and extend the EMG information with a model that describe the essential topology of a single section of the forearm. The way the model is created is intuitive and can be done with the use of freely available software. Once the model is created the computational burden required to perform the calculation is very low and time-wise the processing can be done withing the constraints given by the electromechanical delay. The method is directly created from a high resolution image of the anatomy of the person, creating a network based on information that could be directly verified anytime from the imaging data. This makes the proposed simple, intuitive and highly and easily customizable to people and to conditions.

The position of the electrodes has an influence on the performance of the methods, and the removal of some of them can bring to the degradation of the methods performance. The number of electrodes in the study proposed was maintained over or equal in the worst case to the number of muscles identified on the selected MRI slice in order to keep to problem to become under-determined. Interestingly, the position of the electrodes mostly influencing the performance is not always found to be directly on the involved muscles, but counter intuitively electrodes on the opposite sides seems to have a role in the quality of the estimation.

The validation process still represent a challenging point for the full proof of the results. However the utilized indirect methods provide a good feedback, allowing from one side to evaluate the amount of information utilized and from the other side to evaluate the meaning of the muscle patterns based on well renown anatomical knowledge. An additional method that aim to complements those utilized was

proposed. It utilizes the EMS to provides a simple way to corroborate the system matrix, feeding the system with a known input to verify the nature of the output measured on the electrodes. The experiment described was done with a commercially available EMS system, therefore without the need of specialized. devices.

The extension to the dynamic case, with the application of the method on non-isometric movements to estimate the time varying muscle activation patterns showed that the method can estimate muscle activation patterns according to the anatomy while maintaining a good fitting over the experimental data. Furthermore the methods highlight the presence of phenomena typical of motor control such as co-contractions of muscles. However the low pass nature of the windowing is hindering the possibility to clearly distinguish the activation timing of the agonists and antagonists.

Even though the method as presented in this thesis showed promising results both for isometric and non-isometric tasks, it does not come without limitations and there is still plenty of room for possible changes to improve its quality, performance and robustness.

Even though the re-projection on the electrodes' space and the comparison with the anatomical knowledge from literature provide an goodness index for the method, and the application of the EMS allows to obtain further information, the validation of the method still remains a point that needs to be fully clarified. A direct validation would be impossible. In fact the use of invasive methods such as the intramuscular EMG to gather information from deep muscles would only provide information local to the electrodes's position without providing an overall index of the muscle activation. Furthermore, for body parts, such as the forearm, it would require the

application of a considerable number of needles with a consequent discomfort for the person. However alternative methods can be used to non-invasively access the muscle set with a time resolution closer to that of EMG such as the ultrasounds. Ultrasound could in fact be used during the execution of tasks to have a real time image of the section of target muscles at a high time resolution. In particular using the ultrasounds it would be possible to capture the thickness changes in all muscles, including deep ones. Studies investigated the relation between the thickness of muscles and their activation[80, 81] providing a direct mean to validate the results. Another possible indirect validation could be obtained with the aid of tools such as musculoskeletal modeling and simulations, even if the strong subjectivity of the muscle pattern activation is a point that makes the problem of a solid validation through a general simulated model very challenging.

One important limitation of the method is the fact that it require an MRI scan to obtain morphological information about the anatomic structure, the arrangement and size of the muscles. Even if MRI is now a common technique, it still require time to be collected and the presence of specialized clinical personnel. Furthermore it cannot be taken in case of subjects with pacemakers, cochlear implants or any other iron based implants. Possible solutions might be the use of other faster ways to create a model, such as ultrasounds and computer tomography. Even though they would significantly decreasing the scanning time, they would still require the presence of clinical staff for the scan session. Another solution would be the creation of a template MRI of the anatomical part involved, taking the realistic assumption that the position of the muscle is the same in every person, varying parameters such as the size of the muscle or the amount of fat with direct measurements or with the

use of index that indicates, for example, the level of training that a person has.

6.2 Possible applications and future works

A lot of possible direction could be taken with this research, either for an optimization of the method, or for possible application in different fields related to clinical and rehabilitation practice.

From the side of the improvements, one important point would be the increasing of the participants pool. Even though the number of subjects did not hinder the drawing of any conclusions, it would be important to extend to study to a broader pool of people, in order to have a sample with a bigger variance in terms of subjective activation and also anatomical characteristic for a same body part.

I believe that this method could provide an information that might reveal useful for robotics application. It provides a simple way to extract muscles' information that could be, for example, fed to microstimulators injected inside the muscle, to provide a more physiologically meaningful stimulation of muscles for patients with neurological impairment. Possible others applications can be also considered in the field of rehabilitation robotics, for example to assess the muscle stimulation during repeated movements in order to provide a continuous feedback to therapists supervising the treatment.

Finally, I believe that this method can be a valid way for overcoming the limitations of the previously discussed mfMRI, allowing the estimation of muscle activation with a temporal resolution that would improve the information quality for clinicians in the diagnostic process. In particular, we believe that the proposed method can

make an important contribution in the field of clinical rehabilitation allowing to track muscle activation pattern on impaired subject during rehabilitative cycles considering the underlying morphology of the patient and eventual changes that might happen over time due to a pathological situation. The proposed model relies completely on anatomical and physiological information and is therefore easy to understand for clinical personnel, providing results that are giving a direct quantification of the muscle activation. The dimensions of the model are low and this allow a fast estimation process, potentially allowing a real time tracking of the muscle activity, once the model is created from the subject MRI. For this reason, it is a suitable method to achieve a general overview of the neuromuscular system activation status during rehabilitative exercises and therapies, potentially allowing therapists to assess the reaction and the effectiveness of the rehabilitation strategy on the patients.

Bibliography

- [1] E. Piovanelli, D. Piovesan, S. Shirafuji, B. Su, N. Yoshimura, Y. Ogata, and J. Ota, “Towards a simplified estimation of muscle activation pattern from MRI and EMG using electrical network and graph theory,” *Sensors (Switzerland)*, vol. 20, no. 3, pp. 1–20, 2020, ISSN: 14248220. DOI: 10.3390/s20030724.
- [2] ———, “Influence of the Number and Position of the Electrodes in the Estimation of Muscle Activation Patterns,” *draft*, 2020.
- [3] E. Piovanelli, D. Piovesan, S. Shirafuji, N. Yoshimura, Y. Ogata, and J. Ota, “Muscle Activation Patterns Estimation during Repeated Wrist Movements from MRI and sEMG,” in *The 8th IEEE RAS/EMBS International Conference on Biomedical Robotics and Biomechatronics (BioRob)*, 2020.
- [4] E. Piovanelli, D. Piovesan, S. Shirafuji, and J. Ota, “A Simple Method to Estimate Muscle Currents from HD-sEMG and MRI using Electrical Network and Graph Theory,” in *2019 41st Annual International Conference of the IEEE Engineering in Medicine and Biology Society (EMBC)*, IEEE, 2019, pp. 2657–2662, ISBN: 9781538613115. DOI: 10.1109/embc.2019.8856616.
- [5] ———, “Estimating Deep Muscles Activation from High Density Surface EMG using Graph Theory,” in *2019 IEEE 16th International Conference on Rehabilitation Robotics (ICORR)*, IEEE, 2019, pp. 3–8, ISBN: 9781728127552.
- [6] E. Piovanelli, S. Shirafuji, Y. Ogata, N. Yoshimura, and J. Ota, “sEMG source localization on a three-dimensional model using a Bayesian method: a simulation study,” in *2018 Proceedings of the 2nd International Symposium on Embodied-Brain Systems Science (EmboSS). Osaka, Japan, December 5-6, 2018.*, 2018, p. 36.

- [7] E. Piovaneli, S. Shirafuji, Y. Ogata, Y. Yoshimura, and J. Ota, “A simulation study for visualizing sEMG sources using a Bayesian framework,” in *Proceedings of 40th Annual International Conference of the IEEE Engineering in Medicine and Biology Society (EMBC), July 17-21, 2018, Hawaii, U.S.A.*, 2018.
- [8] K. Fujikawa, S. Shirafuji, B. Su, E. Piovaneli, and J. Ota, “Estimation of fingertip forces using high-density surface electromyography,” in *2017 International Symposium on Micro-NanoMechatronics and Human Science (MHS)*, 2017, pp. 1–5.
- [9] F. Negro, S. Muceli, A. M. Castronovo, A. Holobar, and D. Farina, “Multi-channel intramuscular and surface EMG decomposition by convolutive blind source separation,” *Journal of Neural Engineering*, vol. 13, no. 2, 2016, ISSN: 17412552. DOI: 10.1088/1741-2560/13/2/026027.
- [10] M. Sartori, G. Durandau, S. Dosen, and D. Farina, “Robust Simultaneous Myoelectric Control of Multiple Degrees of Freedom in Wrist-Hand Prostheses by Real-Time Neuromusculoskeletal Modeling,” *Journal of Neural Engineering*, vol. 15, no. 6, 2018.
- [11] C. Son, S. Kim, S. jong Kim, J. Choi, and D. E. Kim, “Detection of muscle activation through multi-electrode sensing using electrical stimulation,” *Sensors and Actuators, A: Physical*, vol. 275, pp. 19–28, 2018, ISSN: 09244247. DOI: 10.1016/j.sna.2018.03.030. [Online]. Available: <https://doi.org/10.1016/j.sna.2018.03.030>.
- [12] T. E. M. Etienne Burdet David W. Franklin, *Human Robotics: Neuromechanics and Motor Control*. Cambridge, Massachusetts : The MIT Press, 2013.
- [13] D. Richfield, *"medical gallery of david richfield 2014"*, 2004. DOI: 10.15347/wjm/2014.009..
- [14] J. L. Dideriksen, D. Farina, and R. M. Enoka, “Influence of fatigue on the simulated relation between the amplitude of the surface electromyogram and muscle force,” *Philosophical Transactions of the Royal Society A: Mathematical, Physical and Engineering Sciences*, vol. 368, no. 1920, pp. 2765–2781, 2010, ISSN: 1364503X. DOI: 10.1098/rsta.2010.0094.
- [15] M. Hodgson, D. Docherty, and D. Robbins, “Post-Activation Potentiation Motor Performance,” vol. 35, no. 7, pp. 585–595, 2005.

- [16] C. J. Heckman and R. M. Enoka, "Motor unit," *Comprehensive Physiology*, vol. 2, no. 4, pp. 2629–2682, 2012, ISSN: 20404603. DOI: 10.1002/cphy.c100087.
- [17] C. K. Thomas, G. Nelson, L. Than, and I. Zijdwind, "Motor unit activation order during electrically evoked contractions of paralyzed or partially paralyzed muscles," *Muscle and Nerve*, vol. 25, no. 6, pp. 797–804, 2002, ISSN: 0148639X. DOI: 10.1002/mus.10111.
- [18] T. A. Kayagil, J. P. Grimes, and W. M. Grill, "Mechanisms underlying reversal of motor unit activation order in electrically evoked contractions after spinal cord injury," *Muscle and Nerve*, vol. 37, no. 2, pp. 210–218, 2008, ISSN: 0148639X. DOI: 10.1002/mus.20914.
- [19] A. V. Hill, "The heat of shortening and the dynamic constants of muscle," *R. Soc. Lond.*, vol. 126, no. 843, pp. 136–195, 1938.
- [20] D. G. Thelen, "Adjustment of Muscle Mechanics Model Parameters to Simulate Dynamic Contractions in Older Adults," *Journal of Biomechanical Engineering*, vol. 125, no. 1, pp. 70–77, Feb. 2003, ISSN: 0148-0731. DOI: 10.1115/1.1531112. eprint: https://asmedigitalcollection.asme.org/biomechanical/article-pdf/125/1/70/5481649/70_1.pdf. [Online]. Available: <https://doi.org/10.1115/1.1531112>.
- [21] M. Millard, T. Uchida, A. Seth, and S. L. Delp, "Flexing Computational Muscle: Modeling and Simulation of Musculotendon Dynamics," *Journal of Biomechanical Engineering*, vol. 135, no. 2, Feb. 2013, 021005, ISSN: 0148-0731. DOI: 10.1115/1.4023390. eprint: https://asmedigitalcollection.asme.org/biomechanical/article-pdf/135/2/021005/6088853/bio_135_2_021005.pdf. [Online]. Available: <https://doi.org/10.1115/1.4023390>.
- [22] S. L. Delp, F. C. Anderson, A. S. Arnold, P. Loan, A. Habib, C. T. John, E. Guendelman, and D. G. Thelen, "Opensim: Open-source software to create and analyze dynamic simulations of movement," *IEEE Transactions on Biomedical Engineering*, vol. 54, no. 11, pp. 1940–1950, 2007.
- [23] E. A. Keshner, D. Campbell, R. T. Katz, and B. W. Peterson, "Neck muscle activation patterns in humans during isometric head stabilization," *Experimental Brain Research*, vol. 75, no. 2, pp. 335–344, 1989, ISSN: 00144819. DOI: 10.1007/BF00247939.

- [24] A. D'Avella, P. Saltiel, and E. Bizzi, "Combinations of muscle synergies in the construction of a natural motor behavior," *Nature Neuroscience*, vol. 6, no. 3, pp. 300–308, 2003, ISSN: 10976256. DOI: 10.1038/nn1010.
- [25] E. Bizzi and V. C. Cheung, "The neural origin of muscle synergies," *Frontiers in Computational Neuroscience*, vol. 7, no. April, pp. 1–6, 2013, ISSN: 16625188. DOI: 10.3389/fncom.2013.00051.
- [26] T. Takei, J. Confais, S. Tomatsu, T. Oya, and K. Seki, "Neural basis for hand muscle synergies in the primate spinal cord," *Proceedings of the National Academy of Sciences of the United States of America*, vol. 114, no. 32, pp. 8643–8648, 2017, ISSN: 10916490. DOI: 10.1073/pnas.1704328114.
- [27] J. J. Kutch and F. J. Valero-Cuevas, "Challenges and new approaches to proving the existence of muscle synergies of neural origin," *PLoS Computational Biology*, vol. 8, no. 5, 2012, ISSN: 1553734X. DOI: 10.1371/journal.pcbi.1002434.
- [28] R. Merletti and D. Farina, *Surface electromyography: physiology, engineering, and applications*, R. Merletti and D. Farina, Eds. John Wiley & Sons Inc, 2016.
- [29] R. Merletti, A. Holobar, and D. Farina, "Analysis of motor units with high-density surface electromyography," *Journal of Electromyography and Kinesiology*, vol. 18, no. 6, pp. 879–890, 2008, ISSN: 10506411. DOI: 10.1016/j.jelekin.2008.09.002.
- [30] D. Leonardis, M. Barsotti, C. Loconsole, M. Solazzi, M. Troncossi, C. Mazzotti, V. P. Castelli, C. Procopio, G. Lamola, C. Chisari, M. Bergamasco, and A. Frisoli, "An EMG-controlled robotic hand exoskeleton for bilateral rehabilitation," *IEEE Transactions on Haptics*, vol. 8, no. 2, pp. 140–151, 2015, ISSN: 19391412. DOI: 10.1109/TOH.2015.2417570.
- [31] D. Farina, E. Fortunato, and R. Merletti, "Noninvasive estimation of motor unit conduction velocity distribution using linear electrode arrays," *IEEE Transactions on Biomedical Engineering*, vol. 47, no. 3, pp. 380–388, 2000.
- [32] L. Mesin, R. Merletti, and A. Rainoldi, "Surface emg: The issue of electrode location," *Journal of Electromyography and Kinesiology*, vol. 19, no. 5, pp. 719–726, 2009, ISSN: 1050-6411. DOI: <https://doi.org/10.1016/j.jelekin.2008.07.006>. [Online]. Available: <http://www.sciencedirect.com/science/article/pii/S1050641108001181>.

- [33] R. H. Chowdhury, M. B. Reaz, M. A. Bin Mohd Ali, A. A. Bakar, K. Chellappan, and T. G. Chang, "Surface electromyography signal processing and classification techniques," *Sensors (Switzerland)*, vol. 13, no. 9, pp. 12 431–12 466, 2013, ISSN: 14248220. DOI: 10.3390/s130912431.
- [34] L. ArendtNielsen, K. R. Mills, and A. Forster, "Changes in muscle fiber conduction velocity, mean power frequency, and mean EMG voltage during prolonged submaximal contractions," *Muscle & Nerve*, vol. 12, no. 6, pp. 493–497, 1989, ISSN: 10974598. DOI: 10.1002/mus.880120610.
- [35] A. Gallina and A. Botter, "Spatial localization of electromyographic amplitude distributions associated to the activation of dorsal forearm muscles," *Frontiers in Physiology*, vol. 4 DEC, no. December, pp. 1–8, 2013, ISSN: 1664042X. DOI: 10.3389/fphys.2013.00367.
- [36] D. Farina, R. Merletti, and R. M. Enoka, "The extraction of neural strategies from the surface EMG," *Journal of Applied Physiology*, vol. 96, no. 4, pp. 1486–1495, 2004, ISSN: 87507587. DOI: 10.1152/japplphysiol.01070.2003.
- [37] C. Disselhorst-Klug, "Improvement of spatial resolution in surface-EMG: A theoretical and experimental comparison of different spatial filters," *IEEE Transactions on Biomedical Engineering*, vol. 44, no. 7, pp. 567–574, 1997, ISSN: 00189294. DOI: 10.1109/10.594897.
- [38] A. Holobar and D. Zazula, "Multichannel blind source separation using convolution Kernel compensation," *IEEE Transactions on Signal Processing*, vol. 55, no. 9, pp. 4487–4496, 2007, ISSN: 1053587X. DOI: 10.1109/TSP.2007.896108.
- [39] A. Holobar, D. Farina, M. Gazzoni, R. Merletti, and D. Zazula, "Estimating motor unit discharge patterns from high-density surface electromyogram," *Clinical Neurophysiology*, vol. 120, no. 3, pp. 551–562, 2009, ISSN: 13882457. DOI: 10.1016/j.clinph.2008.10.160. [Online]. Available: <http://dx.doi.org/10.1016/j.clinph.2008.10.160>.
- [40] A. Holobar and D. Zazula, "Gradient convolution kernel compensation applied to surface electromyograms," *Lecture Notes in Computer Science (including subseries Lecture Notes in Artificial Intelligence and Lecture Notes in Bioinformatics)*, vol. 4666 LNCS, pp. 617–624, 2007, ISSN: 03029743. DOI: 10.1007/978-3-540-74494-8_77.

- [41] M. Chen and P. Zhou, "A novel framework based on FastICA for high density surface EMG decomposition," *IEEE Transactions on Neural Systems and Rehabilitation Engineering*, vol. 24, no. 1, pp. 117–127, 2016, ISSN: 15344320. DOI: 10.1109/TNSRE.2015.2412038.
- [42] A. Holobar, M. A. Minetto, A. Botter, F. Negro, and D. Farina, "Experimental analysis of accuracy in the identification of motor unit spike trains from high-density surface EMG," *IEEE Transactions on Neural Systems and Rehabilitation Engineering*, vol. 18, no. 3, pp. 221–229, 2010, ISSN: 15344320. DOI: 10.1109/TNSRE.2010.2041593.
- [43] M. Sartori, D. G. Llyod, and D. Farina, "Neural data-driven musculoskeletal modeling for personalized neurorehabilitation technologies," *IEEE Transactions on Biomedical Engineering*, vol. 63, no. 5, pp. 879–893, 2016, ISSN: 15582531. DOI: 10.1109/TBME.2016.2538296.
- [44] D. Farina, I. Vujaklija, M. Sartori, T. Kapelner, F. Negro, N. Jiang, K. Bergmeister, A. Andalib, J. Principe, and O. C. Aszmann, "Man/machine interface based on the discharge timings of spinal motor neurons after targeted muscle reinnervation," *Nature Biomedical Engineering*, vol. 1, no. 2, 2017, ISSN: 2157846X. DOI: 10.1038/s41551-016-0025.
- [45] T. Kapelner, M. Sartori, F. Negro, and D. Farina, "Neuro-Musculoskeletal Mapping for Man-Machine Interfacing," *Scientific Reports*, vol. 10, no. 1, p. 5834, 2020, ISSN: 2045-2322. DOI: 10.1038/s41598-020-62773-7. [Online]. Available: <http://www.nature.com/articles/s41598-020-62773-7>.
- [46] B. Cagnie, J. Elliott, S. O’Leary, R. D’Hooge, N. Dickx, and L. Danneels, "Muscle functional MRI as an imaging tool to evaluate muscle activity," *Journal of Orthopaedic and Sports Physical Therapy*, vol. 41, no. 11, pp. 896–903, 2011, ISSN: 01906011. DOI: 10.2519/jospt.2011.3586.
- [47] t. f. e. Wikipedia. (), [Online]. Available: https://en.wikipedia.org/wiki/Main_Page.
- [48] R. A. Meyer and B. M. Prior, "Functional magnetic resonance imaging of muscle," *Exercise and Sport Sciences Reviews*, vol. 28, no. 2, pp. 89–92, 2000, ISSN: 00916331.

- [49] J. M. Mayer, J. E. Graves, B. C. Clark, M. Formikell, and L. L. Ploutz-Snyder, "The use of magnetic resonance imaging to evaluate lumbar muscle activity during trunk extension exercise at varying intensities," *Spine*, vol. 30, no. 22, pp. 2556–2563, 2005, ISSN: 03622436. DOI: 10.1097/01.brs.0000186321.24370.4b.
- [50] N. Dickx, R. D’Hooge, B. Cagnie, E. Deschepper, K. Verstraete, and L. Dancneels, "Magnetic resonance imaging and electromyography to measure lumbar back muscle activity," *Spine*, vol. 35, no. 17, pp. 836–842, 2010, ISSN: 03622436. DOI: 10.1097/BRS.0b013e3181d79f02.
- [51] R. Kinugasa and H. Akima, "Neuromuscular activation of triceps surae using muscle functional MRI and EMG," *Medicine and Science in Sports and Exercise*, vol. 37, no. 4, pp. 593–598, 2005, ISSN: 01959131. DOI: 10.1249/01.MSS.0000159026.99792.76.
- [52] M. Kumagai, N. Shiba, F. Higuchi, H. Nishimura, and A. Inoue, "Functional evaluation of hip abductor muscles with use of magnetic resonance imaging," *Journal of Orthopaedic Research*, vol. 15, no. 6, pp. 888–893, 1997, ISSN: 07360266. DOI: 10.1002/jor.1100150615.
- [53] G. R. Adams, M. R. Duvoisin, and G. A. Dudley, "Magnetic resonance imaging and electromyography as indexes of muscle function," *Journal of Applied Physiology*, vol. 73, no. 4, pp. 1578–1583, 1992, ISSN: 01617567. DOI: 10.1152/jappl.1992.73.4.1578.
- [54] T. B. Price, G. Kamen, B. M. Damon, C. A. Knight, B. Applegate, J. C. Gore, K. Eward, and J. F. Signorile, "Comparison of MRI with EMG to study muscle activity associated with dynamic plantar flexion," *Magnetic Resonance Imaging*, vol. 21, no. 8, pp. 853–861, 2003, ISSN: 0730725X. DOI: 10.1016/S0730-725X(03)00183-8.
- [55] M. Fisher, R. A. Meyer, G. R. Adams, J. M. Foley, and E. Potchen, "Direct Relationship Between Proton T2 and Exercise Intensity in Skeletal Muscle MR Images," *Investigative Radiology*, vol. 25, pp. 480–485, 1990.
- [56] F. Hug, K. Tucker, J.-L. Gennisson, M. Tanter, and A. Nordez, "Elastography for Muscle Biomechanics : Toward the Estimation of Individual Muscle Force," *Exercise and Sports Sciences Reviews*, vol. 43, no. 3, pp. 125–133, 2015. DOI: 10.1249/JES.0000000000000049.

- [57] K. Bouillard and A. Nordez, "Estimation of Individual Muscle Force Using Elastography," vol. 6, no. 12, 2011. DOI: 10.1371/journal.pone.0029261.
- [58] Y. Nakajima, S. Keeratihattayakorn, S. Yoshinari, and S. Tadano, "An emg-ct method using multiple surface electrodes in the forearm," *Journal of Electromyography and Kinesiology*, vol. 24, pp. 875–880, 2014.
- [59] B. Su, S. Shirafuji, T. Oya, Y. Ogata, T. Funato, N. Yoshimura, L. Pion-Tonachini, S. Makeig, K. Seki, and J. Ota, "Source separation and localization of individual superficial forearm extensor muscles using high-density surface electromyography," in *2016 International Symposium on Micro-NanoMechatronics and Human Science, MHS 2016*, 2017, pp. 1–7, ISBN: 9781509027842. DOI: 10.1109/MHS.2016.7824149.
- [60] E. L. Nussbaum, P. Houghton, J. Anthony, S. Rennie, B. L. Shay, and A. M. Hoens, "Neuromuscular electrical stimulation for treatment of muscle impairment: Critical review and recommendations for clinical practice," *Physiotherapy Canada*, vol. 69, no. 5 Special Issue, pp. 1–76, 2017, ISSN: 03000508. DOI: 10.3138/ptc.2015-88.
- [61] N. A. Maffiuletti, M. A. Minetto, D. Farina, and R. Bottinelli, "Electrical stimulation for neuromuscular testing and training: State-of-the art and unresolved issues," *European Journal of Applied Physiology*, vol. 111, no. 10, pp. 2391–2397, 2011, ISSN: 14396319. DOI: 10.1007/s00421-011-2133-7.
- [62] G. E. Loeb, R. A. Peck, W. H. Moore, and K. Hood, "BION system for distributed neural prosthetic interfaces," *Medical Engineering and Physics*, vol. 23, no. 1, pp. 9–18, 2001, ISSN: 13504533. DOI: 10.1016/S1350-4533(01)00011-X.
- [63] T. K. Whitehurst, J. H. Schulman, K. N. Jaax, and R. Carbunaru, "The bionō microstimulator and its clinical applications," in *Implantable Neural Prostheses 1: Devices and Applications*, E. Greenbaum and D. Zhou, Eds. New York, NY: Springer US, 2009, pp. 253–273, ISBN: 978-0-387-77261-5. DOI: 10.1007/978-0-387-77261-5_8. [Online]. Available: https://doi.org/10.1007/978-0-387-77261-5_8.
- [64] G.I. Atabekov, *Linear Network Theory*. Pergamon Press, 1965.

- [65] F. Dorfler, J. W. Simpson-Porco, and F. Bullo, "Electrical Networks and Algebraic Graph Theory: Models, Properties, and Applications," *Proceedings of the IEEE*, vol. 106, no. 5, pp. 977–1005, 2018, ISSN: 00189219. DOI: 10.1109/JPR0C.2018.2821924. eprint: arXiv:0908.2426v2.
- [66] C. A. Schneider, W. S. Rasband, and K. W. Eliceri, "NIH Image to ImageJ: 25 years of Image Analysis," *Nature Methods*, vol. 9, no. 7, pp. 671–675, 2012. DOI: 10.1007/978-1-84882-087-6_9.
- [67] V. K. Kikinis R Pieper SD, "3d slicer: A platform for subject-specific image analysis, visualization, and clinical support," in *Intraoperative Imaging Image-Guided Therapy*, F. A. Jolesz, Ed., pp. 277–289.
- [68] B. K. P. Horn, "Closed-form solution of absolute orientation using unit quaternions," *Journal of the Optical Society of America A*, no. 4, pp. 629–642, 1987.
- [69] M. M. Lowery, N. S. Stoykov, J. P. A. Dewald, and T. A. Kuiken, "Volume Conduction in an Anatomically Based Surface EMG Model," *IEEE Transactions on Biomedical Engineering*, vol. 51, no. 12, pp. 2138–2147, 2004, ISSN: 0018-9294. DOI: 10.1109/TBME.2004.836494. [Online]. Available: <http://ieeexplore.ieee.org/lpdocs/epic03/wrapper.htm?arnumber=1360033>.
- [70] A.I.Kapandji, *The Physiology of the Joints. 1. The Upper limb, 7th Edition*. Handspring Publishing, 2019.
- [71] W.Platzer, *Color Atlas of Human Anatomy, Vol.1 Locomotor System, 7th Edition*. Thieme, 2015.
- [72] M. Kristiansen, P. Madeleine, E. A. Hansen, and A. Samani, "Inter-subject variability of muscle synergies during bench press in power lifters and untrained individuals," *Scandinavian Journal of Medicine and Science in Sports*, vol. 25, no. 1, pp. 89–97, 2015, ISSN: 16000838. DOI: 10.1111/sms.12167.
- [73] F. Hug, D. Bendahan, Y. Le Fur, P. J. Cozzone, and L. Grélot, "Heterogeneity of muscle recruitment pattern during pedaling in professional road cyclists: A magnetic resonance imaging and electromyography study," *European Journal of Applied Physiology*, vol. 92, no. 3, pp. 334–342, 2004, ISSN: 14396319. DOI: 10.1007/s00421-004-1096-3.
- [74] R. C. Araujo, M. Duarte, and A. C. Amadio, *On the inter- and intra-subject variability of the electromyographic signal in isometric contractions*, 2000.

- [75] Edwards RG and Lippold OC, "The Relation Between Force and Electrical Activity in Fatigued Muscle," *The Journal of Physiology*, no. 132, pp. 677–681, 1956. [Online]. Available: <http://www.saburchill.com/physics/chapters/0009b.html>.
- [76] M. Naeije and H. Zorn, "Relation between EMG power spectrum shifts and muscle fibre action potential conduction velocity changes during local muscular fatigue in man," *European Journal of Applied Physiology and Occupational Physiology*, vol. 50, no. 1, pp. 23–33, 1982, ISSN: 03015548. DOI: 10.1007/BF00952241.
- [77] T. Moritani, A. Nagata, and M. Muro, *Electromyographic manifestations of muscular fatigue*, 1982. DOI: 10.1249/00005768-198203000-00008.
- [78] S. C. Gandevia, "Spinal and supraspinal factors in human muscle fatigue," *Physiological Reviews*, vol. 81, no. 4, pp. 1725–1789, 2001, ISSN: 00319333. DOI: 10.1152/physrev.2001.81.4.1725.
- [79] E. A. Clancy, C. Martinez-Luna, M. Wartenberg, C. Dai, and T. R. Farrell, "Two degrees of freedom quasi-static EMG-force at the wrist using a minimum number of electrodes," *Journal of Electromyography and Kinesiology*, vol. 34, pp. 24–36, 2017. DOI: 10.1016/j.physbeh.2017.03.040.
- [80] L. Colby Mangum, K. Henderson, K. P. Murray, and S. A. Saliba, "Ultrasound assessment of the transverse abdominis during functional movement," *Journal of Ultrasound in Medicine*, vol. 37, no. 5, pp. 1225–1231, 2018, ISSN: 15509613. DOI: 10.1002/jum.14466.
- [81] T. Fukunaga, M. Miyatani, M. Tachi, M. Kouzaki, Y. Kawakami, and H. Kanehisa, "Muscle volume is a major determinant of joint torque in humans," *Acta Physiologica Scandinavica*, vol. 172, no. 4, pp. 249–255, 2001, ISSN: 00016772. DOI: 10.1046/j.1365-201X.2001.00867.x.

